Electronic Supplementary Material (ESI) for ChemComm.

Supporting Information for

Au-Pd Bimetallic nanoparticles supported on a high nitrogen-rich ordered mesoporous carbon as an efficient catalyst for room temperature Ullman coupling of aryl chlorides in aqueous media

Babak Karimi*[a,b], Hossein Barzegar[a], and Hojatollah Vali[c]

[a] *Department of Chemistry, Institute for Advanced Studies in Basic Sciences (IASBS), PO-Box 45195-1159, Gava-zang, Zanjan 45137-6731, Iran*

[b] *Research Center for Basic Sciences & Modern Technologies (RBST), Institute for Advanced Studies in Basic Sciences (IASBS), Zanjan 45137-66731, Iran.*

[c] *Department of Anatomy and Cell Biology and Facility for Electron Microscopy Research McGill University; Montreal, Quebec H3A2A7, Canada*

Table of content

1. Experimental

1.1. Characterization

The pore structures of the prepared materials were observed by transmission electron microscopy (Philips CM-200 and Titan Krios TEM). All analysis were performed using KNAUER system equipped with UV K-2600 and RI K-2301 refractive index detectors. N_2 adsorption isotherms were measured at 77 K on Belsorp (BELMAX, Japan) analyzer using standard continuous procedures, and samples were first degassed at 353 K for 5 h. Specific surface area was determined from the linear part of the BET plot ($P/P_0 \approx 0.05$-0.15), the pore size distribution was calculated from the adsorption branch using Barrett–Joyner–Halenda (BJH) method, total pore volume was estimated based on the N_2 adsorbed at $P/P_0 \approx 0.995$. Elemental composition was characterized by an energy dispersive spectrometer (EDS) attached to Philips-TEM. XPS spectra were recorded on Kratos Analytical X-ray photoelectron spectrometers. To correct possible deviation caused by electric charge, the C1s line at 285.0 eV was used as the internal standard. The Nitrogen contents in the carbon materials determined by elemental analysis (vario-EL CHNS instrument). Thermogravimetric analysis was performed by using a NETZSCH STA 409 PC/PG instrument at scan rates of 20 K min^{-1}, with typically 5 mg sample under flowing N_2. Gas chromatography analyses were performed on Varian CP-3800 using a flame ionization detector (FID) using suitable internal standards. NMR spectra were recorded using a Brüker (^1H frequency: 400 MHz, ^{13}C frequency: 100 MHz).

1.2. Chemicals

Pluronic P123 (EO20PO70EO20 (EO= ethyleneoxide, PO= propylene oxide), M_{av}= 5800), tetraethyl orthosilicate (TEOS), sodium tetrachloropalladate ($NaPdCl_4$) and sodium tetrachloroaurate (Na_2AuCl_4) were purchased from Aldrich. 1-Methylimidazole, 2- henylethyl bromide, sodium borohydride, sulfuric acid (95-98 %), hydrochloric acid (37 %) and solvents were obtained from Merck Company and used without purification.

1.3. Synthesis

1.3.1. Preparation of SBA-15

Briefly, 24 g of pluronic P123 ($EO_{20}PO_{70}EO_{20}$ (EO=ethylene oxide, PO= propylene oxide), M_{av}=5800, Aldrich) was dissolved in 505 mL of H_2O and 101 mL of concentrated HCl at 35 ºC. Consequently, tetraethyl orthosilicate (TEOS) (54.2 g) was added to the solution. The mixture was stirred vigorously at 35 ºC for 20 h followed by an aging step at 80 ºC for 24 h. The solid material were separated by filtration, washed with deionized water and dried at room temperature. The surfactant was removed by solvent extraction with anhydrous ethanol in a soxhlet apparatus for 24 h.

1.3.2. Preparation of 1-methyl-3-phenethyl-1H-imidazolium hydrogen sulfate (MPIHS)

1, 3-dialkylimidazolium bromide was prepared according to standard methods and their purities were established before utilization by ^{13}CNMR and ^{1}HNMR. Briefly, a solution of dry toluene (50 mL), 1-methylimidazole (73.1 mmol) and 2-bromo-1-phenylethane (80.3 mmol) was refluxed for 24 h under an argon atmosphere. The resulting two phase reaction mixture was then allowed to cool at room temperature. The separated ionic liquid (IL) layer was washed with dry toluene and dry Et_2O and dried under vacuum. The anion-exchange reaction was carried out in dry methylene chloride containing 1 mmol of 1, 3-dialkylimidazolium bromide and 1 mmol of H_2SO_4. The solution was refluxed for 48 h until any hydrogen bromide by-product was removed. After evaporation of the solvent under vacuum, 1-methyl-3-phenethyl-1H-imidazolium hydrogen sulfate (MPIHS) was isolated in good yield.

1.3.3. Preparation of Ionic Liquid Derived Fibrillated Mesoporous Carbon (IFMC)

The IFMC was prepared through the carbonization of 1-methyl-3-phenethyl-1H-imidazolium hydrogen Sulfate (MPIHS) using ordered mesoporous silica SBA-15 as a template following the reported procedure [B. Karimi, H. Behzadnia, M. Bostina, and H. Vali, *Chem. Eur. J.*, **2012**, *18*, 8634]. At first, in order to deposit MPIHS into the surfactant-free SBA-15 channels, a dry acetonitrile solution of the IL (1 mL of MPIHS in 25 mL of acetonitrile) was added drop wise to a suspension of SBA-15 in acetonitrile. After 24 h of stirring at room temperature, the solvent was removed under reduced pressure. The resulted powdery material

was impregnated with aqueous solution of sulfuric acid (4 g H_2O, 0.14 g H_2SO_4) and placed at 100 °C in a vacuum drying oven for 6 h. Consequently, the oven temperature was increased to 160 °C and maintained for 6 h at that temperature to afford a dark brown powder. 0.4 mL of MPIHS was incorporated again into mesoporous silica hosts by the same procedure. After that, the IL carbonized at 900 ºC for 3 h under a flow of argon atmosphere. Ionic liquid derived Fibrillated Mesoporous Carbon (IFMC) was obtained by dissolving the silica framework in NaOH aqueous solution for 24 h. The resulted carbon was filtered, washed several times with deionized water and ethanol, and dried at the vacuum

1.3.4. Preparation of Nitrogen-doped Ordered Mesoporous Carbon from Iran-1 (NMCI-1)

The NMCI-1 was prepared as follow: At first, 1 mL of MPIHS was heated at 100 ºC and 0.1 g Guanine was added slowly and the mixture was stirred until dissolution of Guanine in IL. In the next step, SBA-15 (1 g) was added slowly to form a SBA-15/IL paste. As described above, the final composite was transferred into oven and carbonization procedure was performed under argon 5 $LMin^{-1}$ at 900 ºC. Subsequently, the hard template was removed by dissolution in a sodium hydroxide (2 M) solution for 24 h at 50 ºC. Filtration of the carbonized NMCI-1 material and washing with deionized water up to neutralizing point and ethanol gives the final NMCI-1 material in ~10 wt % yield with respect to weight of IL and Guanine.

1.3.5. Preparation of Nitrogen-doped Ordered Mesoporous Carbon from Iran-2 (NMCI-2)

The NMCI-2 was prepared as follow: At first, 1 mL of MPIHS was heated at 100 ºC and 0.15 g Guanine was added slowly and the mixture was stirred until dissolution of Guanine in IL. In the next step, SBA-15 (1 g) was added slowly to form a SBA-15/IL paste. As described above, the final composite was transferred into oven and carbonization procedure was performed under argon 5 $LMin^{-1}$ at 900 ºC. Subsequently, the hard template was removed by dissolution in a sodium hydroxide (2 M) solution for 24 h at 50 ºC. Filtration of the carbonized NMCI-2 material and washing with deionized water up to neutralizing point and

ethanol gives the final NMCI-2 material in ~10 wt % yield with respect to weight of IL and Guanine.

1.3.6. Preparation of CMK-3

The template-free SBA-15 material was used as a mold for the synthesis of CMK-3 according to the literatures (Jun, S.; Joo, S. H.; Ryoo, R.; Kruk, M.; Jaroniec, M.; Liu, Z.; Ohsuna, T.; Terasaki, O. *J. Am. Chem. Soc.* **2000**, *122,* 10712-10713.). Typically, the resulted template-free SBA-15 was impregnated with aqueous solution of sucrose (1.25 g of sucrose in 5 g of H_2O) containing 0.14 g of sulfuric acid and placed at 100 °C in a vacuum drying oven for 6 h. Consequently the oven temperature was increased to 160 °C and maintained for 6 h at that temperature to afford a dark brown or black powder. The impregnation step was repeated once with 0.8 g of sucrose. The resulted composite was then kept in an argon flow at 900 °C for 2 h to carbonize the sucrose. Afterward, in order to remove the silica template, the generated black powder was stirred in a solution of ethanol and 1 M sodium hydroxide at 50 °C for 8 h. The CMK-3 carbon was afforded after filtration, washed several times with ethanol, and dried.

1.3.7. Preparation of Au-Pd@NMCI-2

Synthesis of the Mesoporous Carbon-stabilized bimetallic nanoparticles (Au-Pd@NMCI-2) was preformed via reduction of $NaPdCl_4$ and Na_2AuCl_4 with a solution of $NaBH_4$ in milli-Q water. A suspension of NMCI-2 (100 mg) in milli-Q water (20 mL) was sonicated for 30 min. Afterward, 0.026 mmol of $NaPdCl_4$ and 0.026 mmol of Na_2AuCl_4 were dissolved in milli-Q water (20 mL) and added to the NMCI-2 suspension. In order to prepare bimetallic NPs onto NMCI-2, 0.26 mmol of $NaBH_4$ was added into the suspension, which is placed into ice bath, under vigorous stirring. After vigorous stirring for 10 min, Au-Pd@NMCI-2 was afforded after filtration, and dried. The total loading of Au and Pd in the catalyst were 0.085 and 0.238 $mmol.g^{-1}$, respectively (Au/Pd ratio = 2.8/1). This ratio is more or less very close to the ratio of Au/Pd estimated by line-scan energy dispersive X-ray spectroscopy (EDAX) of Au-Pd alloy nanoparticles in the Au-Pd@NMCI-2 (Au/Pd ratio ≅ 4/1) (Figure 3, manuscript)

1.3.8. Preparation of Au-Pd@NMCI-1

Synthesis of the Mesoporous Carbon-stabilized bimetallic nanoparticles (Au-Pd@NMCI-1) was preformed via following the same procedure as it was described for Au-Pd@NMCI-2.

1.3.9. Preparation of Au-Pd@IFMC

Synthesis of the Mesoporous Carbon-stabilized bimetallic nanoparticles (Au-Pd@IFMC) was preformed via following the same procedure as it was described for Au-Pd@NMCI-2.

1.3.10. Preparation of Au-Pd@CMK-3

Synthesis of the Mesoporous Carbon-stabilized bimetallic nanoparticles (Au-Pd@CMK-3) was preformed via following the same procedure as it was described for Au-Pd@NMCI-2.

1.3.11. Preparation of Au-Pd@C

Synthesis of commercial Carbon Active-stabilized bimetallic nanoparticles (Au-Pd@C) was performed via following the same procedure as it was described for Au-Pd@NMCI-2.

1.3.12. Preparation of Au@NMCI-2

Synthesis of the Mesoporous Carbon-stabilized bimetallic nanoparticles (Au@NMCI-2) was preformed via reduction of Na_2AuCl_4 with a solution of $NaBH_4$ in milli-Q water. A suspension of NMCI-2 (50 mg) in milli-Q water (20 mL) was sonicated for 30 min. Afterward, 0.026 mmol of Na_2AuCl_4 was dissolved in milli-Q water (20 mL) and added to the NMCI-2 suspension. In order to prepare Au NPs onto NMCI-2, 0.13 mmol of $NaBH_4$ was added into the suspension, which is placed into ice bath, under vigorous stirring. After vigorous stirring for 10 min, Au@NMCI-2 was afforded after filtration, and dried.

1.3.13. Preparation of Pd@NMCI-2

Synthesis of the Mesoporous Carbon-stabilized bimetallic nanoparticles (Pd@NMCI-2) was preformed via reduction of $NaPdCl_4$ with a solution of $NaBH_4$ in milli-Q water. A suspension of NMCI-2 (50 mg) in milli-Q water (20 mL) was sonicated for 30 min. Afterward, 0.026 mmol of $NaPdCl_4$ was dissolved in milli-Q water (20 mL) and added to the NMCI-2 suspension. In order to prepare Pd NPs onto NMCI-2, 0.13 mmol of $NaBH_4$ was added into

the suspension, which is placed into ice bath, under vigorous stirring. After vigorous stirring for 10 min, Pd@NMCI-2 was afforded after filtration, and dried.

1.3.14. General procedure for the Ullmann coupling reaction

0.25 mmol of aryl halides, 0.7-1.2 mol % of catalyst, 2 mmol of K_2CO_3 and 3 mL mixture of water/ethanol (4:1) were placed in a glass flask. The catalytic reaction was performed at room temperature with vigorous stirring at the desired time. The reaction was monitored by GC and TLC, and after completion of the reaction, the products were separated by simple organic extraction and purified by crystallization. The recyclability of Au-Pd@NMCI-2 was examined by isolating it from the Ullmann reaction of Chlorobenzene in a mixture of water/ethanol (4:1). When the reaction was completed in the first run, the catalyst was recovered by a simple filtration, followed by washing with excess of ethyl acetate. The catalyst was reused directly for the next run. The catalytic activity of Au-Pd@NMCI-2, remained almost constant during five reaction cycles.

1.4. Spectral data for Table 2

4,4'-dimethoxy-1,1'-biphenyl: ^{1}H-NMR (400 MHz; $CDCl_3$; TMS): δ_H = 3.88 (s, 6H), 7.00 (d, *J* = 8.8 Hz, 4H), 7.52 (d, *J* = 8.8 Hz, 4H); ^{13}C-NMR (100 MHz, $CDCl_3$; TMS): 56.21, 115.03, 128.60, 134.35, 159.57.

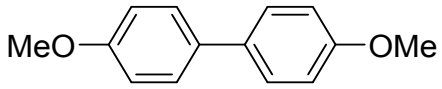

4,4'-dimethyl-1,1'-biphenyl : ^{1}H-NMR (400 MHz; $CDCl_3$; TMS): δ_H = 2.43 (s, 6H), 7.27 (d, *J* = 8.4 Hz, 4H), 7.52 (d, *J* = 8.4 Hz, 4H); ^{13}C-NMR (100 MHz, $CDCl_3$; TMS): δ_C =21.95, 127.66, 130.29, 137.55, 139.14.

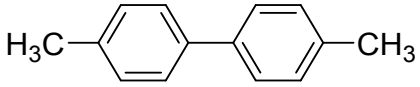

biphenyl: ^{1}H-NMR (400 MHz; $CDCl_3$; TMS): δ_H = 7.40 (t, *J* = 7.2 Hz, 4H), 7.50 (dd, J_1 = 7.2 Hz, J_2 = 8.0 Hz, 4H), 7.65 (d, *J*= 8.0 Hz, 2H); ^{13}C-NMR (100 MHz, $CDCl_3$; TMS): δ_C = 127.4, 127.5, 129.0, 141.4

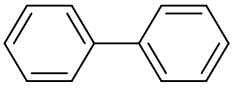

2,2'-bithiophene: ^{1}H-NMR (400 MHz; $CDCl_3$; TMS): δ_H = 7.36-7.39 (m, 4H), 7.41 (dd, J_1= 1.6 Hz, J_2=3.2 Hz, 2H); ^{13}C-NMR (100 MHz, $CDCl_3$; TMS): δ_C =127.0, 127.7, 129.9, 137.2.

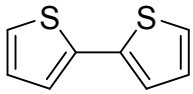

3,3'-bithiophene: ^{1}H-NMR (400 MHz; $CDCl_3$; TMS): δ_H = 7.04 (dd, J_1=5.2 Hz, J_2=3.6 Hz, 2H), 7.09 (dd, J_1=3.6 Hz, J_2=1.2 Hz, 2H), 7.27 (dd, J_1=5.2 Hz, J_2=1.2 Hz, 2H); ^{13}C-NMR (100 MHz, $CDCl_3$; TMS): δ_C =127.0, 127.7, 129.9, 137.2.

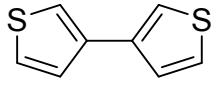

[1,1'-biphenyl]-4,4'-dicarbonitrile: ^{1}H-NMR (400 MHz; $CDCl_3$; TMS): δ_H = 7.73 (d, J = 8.4 Hz, 4H), 7.82 (d, J = 8.4 Hz, 4H); ^{13}C-NMR (100 MHz, $CDCl_3$; TMS): δ_C = 113.3, 119.3, 128.8, 133.7, 144.3.

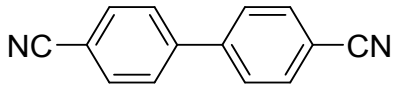

4,4'-dinitro-1,1'-biphenyl: ^{1}H-NMR (400 MHz; $CDCl_3$; TMS): δ_H = 7.82 (d, J = 4.8 Hz, 4 H), 8.42 (d, J = 4.8 Hz, 4 H); ^{13}C-NMR (100 MHz, $CDCl_3$; TMS): δ_C = 125.26, 129.2, 145.8, 148.92.

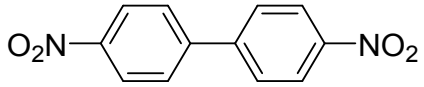

[1,1'-biphenyl]-3,3'-dicarbonitrile: ^{1}H-NMR (400 MHz; $CDCl_3$; TMS): δ_H =7.64 (dd, J_1 = J_2 = 8.0 Hz, 2H), 7.75 (ddd, J_1 = J_2 = 1.2 Hz, J_3 = 8.0 Hz, 2 H), 7.83 (ddd, J_1 = J_2 = 1.2 Hz, J_3 = 8.0 Hz, 2 H), 7.88 (dd, J_1 = J_2 = 1.2 Hz, 2 H)); ^{13}C-NMR (100 MHz, $CDCl_3$; TMS): δ_C =114.3, 119.1, 130.9, 131.5, 132.2, 132.6, 141.0

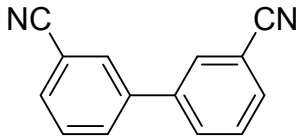

1,1'-([1,1'-biphenyl]-4,4'-diyl)bis(ethan-1-one): ^{1}H-NMR (400 MHz; $CDCl_3$; TMS): δ_H = 2.68 (s, 6H), 7.75 (d, J = 8.4 Hz, 4H), 8.09 (d, J = 8.4 Hz, 4H); ^{13}C-NMR (100 MHz, $CDCl_3$; TMS): 29.77, 127.66, 129.29, 136.55, 144.14, 197.68.

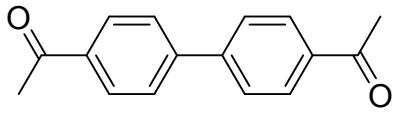

[1,1'-biphenyl]-2,2'-diol: ^{1}H-NMR (400 MHz; $CDCl_3$; TMS): δ_H = 5.58 (S, exchangeable, 2H), 7.08 (dd, J_1=J_2= 8.0 Hz, 2H) ; 7.10 (d, J= 8.0 Hz, 2H); 7.31 (dd, J_1 = 1.6, J_2= 8.0 Hz, 2H), 7.38 (ddd, J_1=1.6 Hz, J_2=J_3= 8.0 Hz, 2H); ^{13}C-NMR (100 MHz, $CDCl_3$; TMS): 119.5, 1224, 124.3, 130.8, 132.1, 153.8.

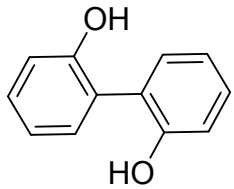

3,3'-dinitro-1,1'-biphenyl: ^{1}H-NMR (400 MHz; $CDCl_3$; TMS): δ_H =7.74 (, J = 8.0 Hz, 2 H), 8.15 (ddt, J_{d1} = 0.8 Hz, J_{d2} = 2.0 Hz J_t = 8 Hz, 2 H), 8.34 (ddt, J_{d1} = 0.8 Hz, J_{d2} = 2.0 Hz J_t = 8 Hz, 2 H),, 8.53 (dd, J_1 =J_2 = 2.0 Hz, 2 H); ^{13}C-NMR (100 MHz, $CDCl_3$; TMS): δ_C =113.0, 124.2, 130.9, 131.2, 133.9, 141.2, 149.7

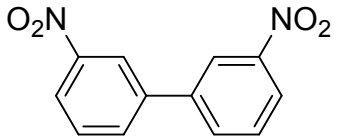

2. Tables

Table S1. Elemental analysis Results for NMCI-2

Material	Sulfur (%)	Oxygen (%)	Carbon (%)	Nitrogen (%)
NMCI-2	1 %	1.5 %	72 %	12.6 %

3. Figures

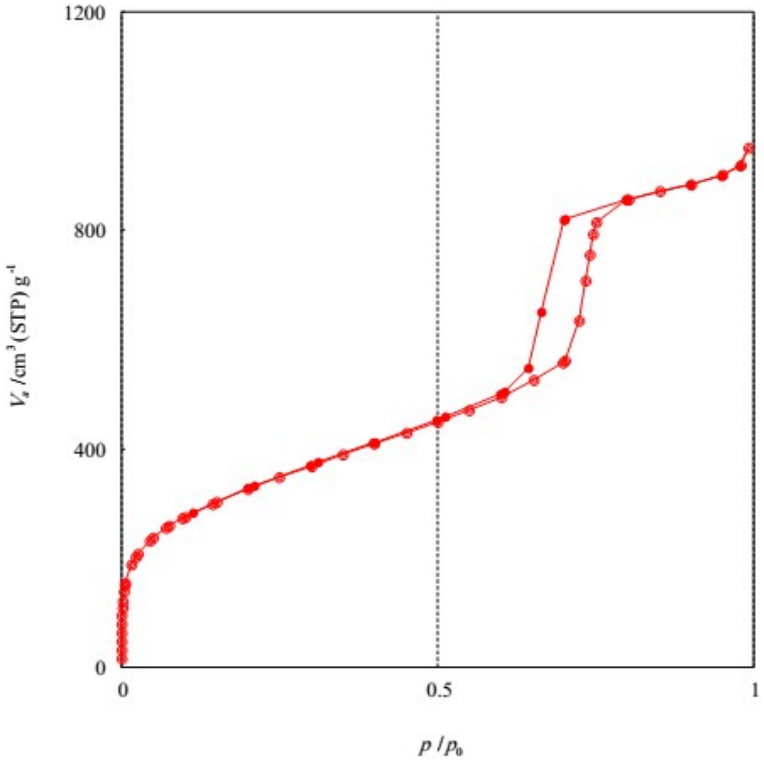

Figure S1. N_2 adsorption-desorption isotherm of SBA-15 [S_{BET} = 1073 m^2 g^{-1} and V_t = 1.40 cm^3 g^{-1}]

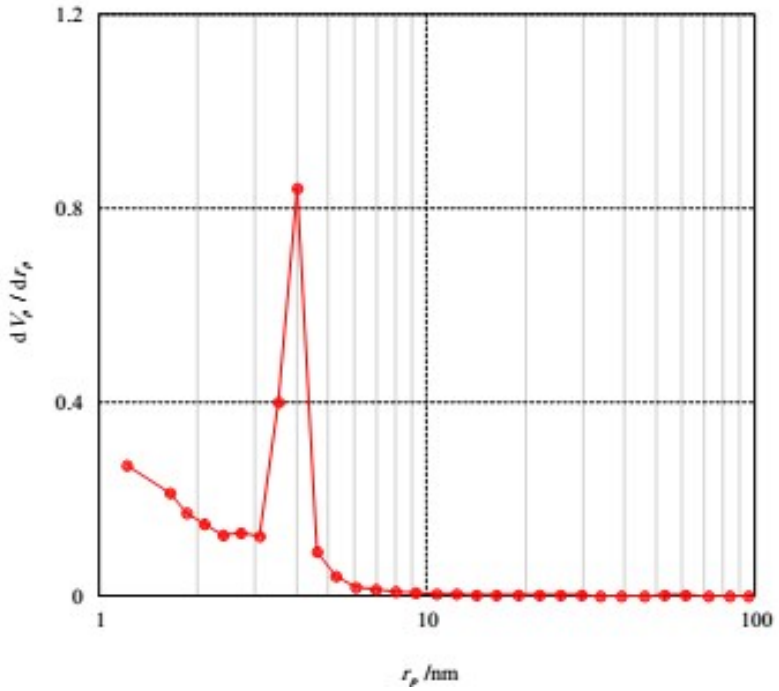

Figure S2. BJH pore size distributions analysis for SBA-15 [D_{BJH} = 8.06 nm]

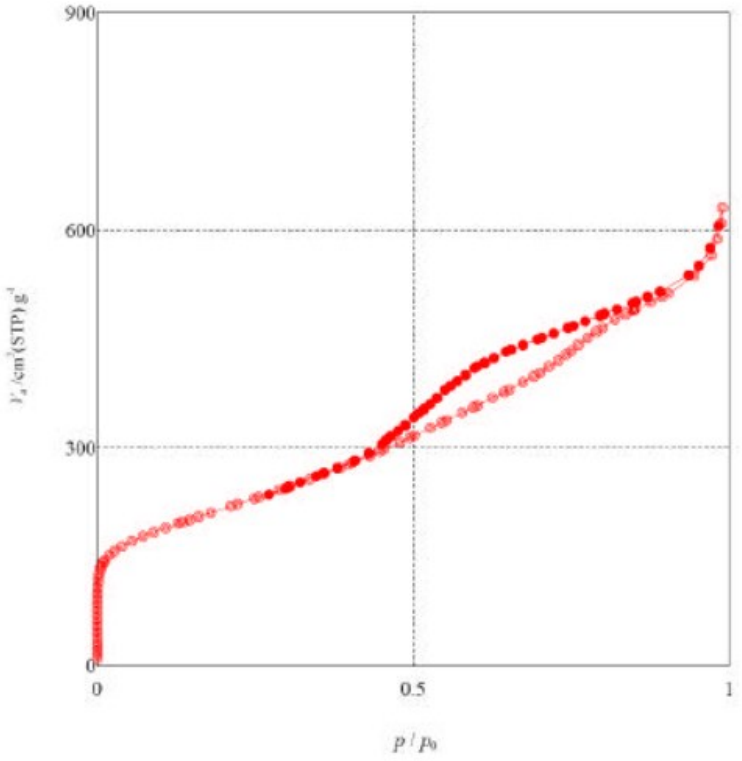

Figure S3. N_2 adsorption-desorption isotherm of IFMC [S_{BET} = 778 m^2 g^{-1} and V_t = 0.98 cm^3 g^{-1}]

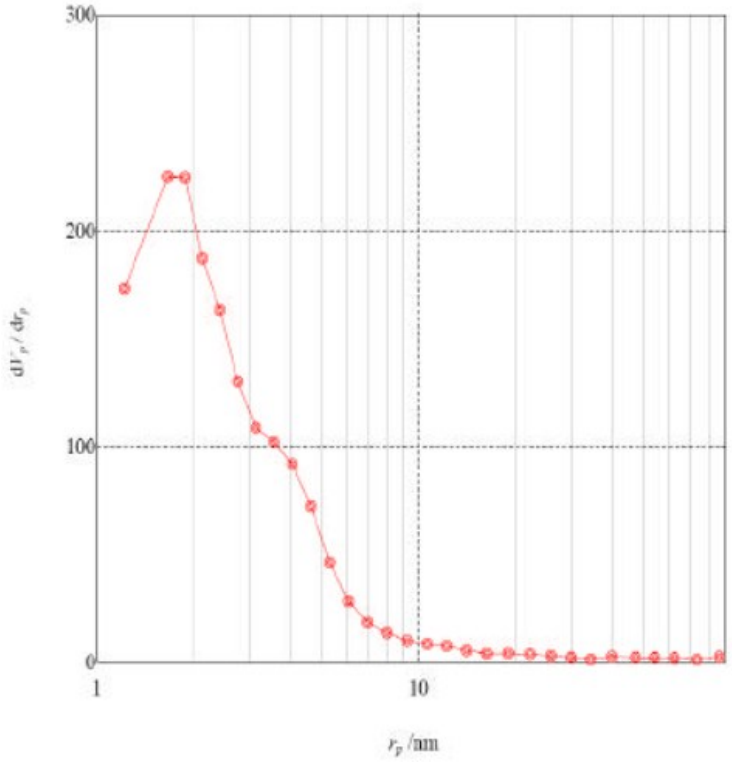

Figure S4. BJH pore size distributions analysis for IFMC [D_{BJH} = 3.32 nm]

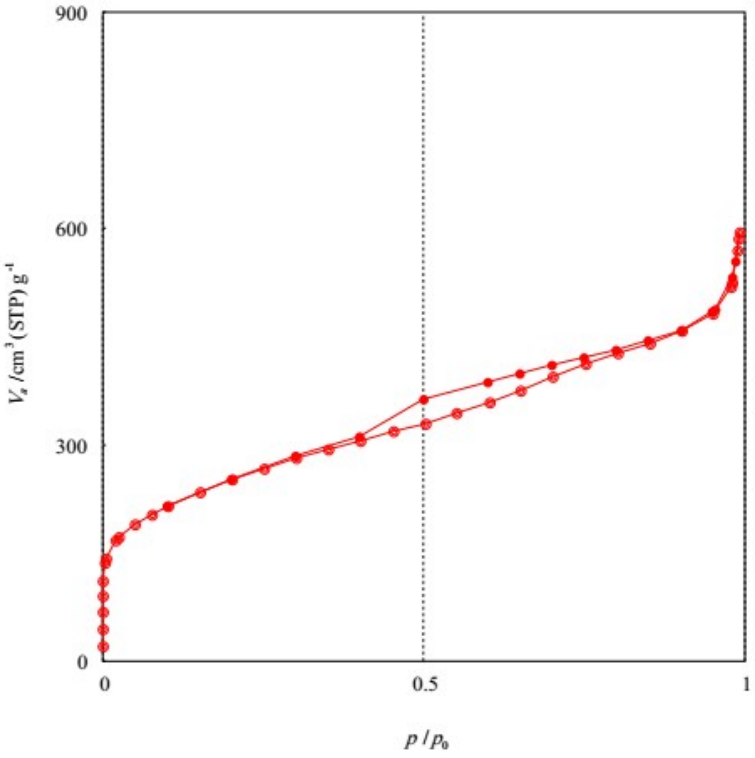

Figure S5. N_2 adsorption-desorption isotherm of NMCI-1 [S_{BET} = 900 m^2 g^{-1} and V_t = 0.9 cm^3 g^{-1}]

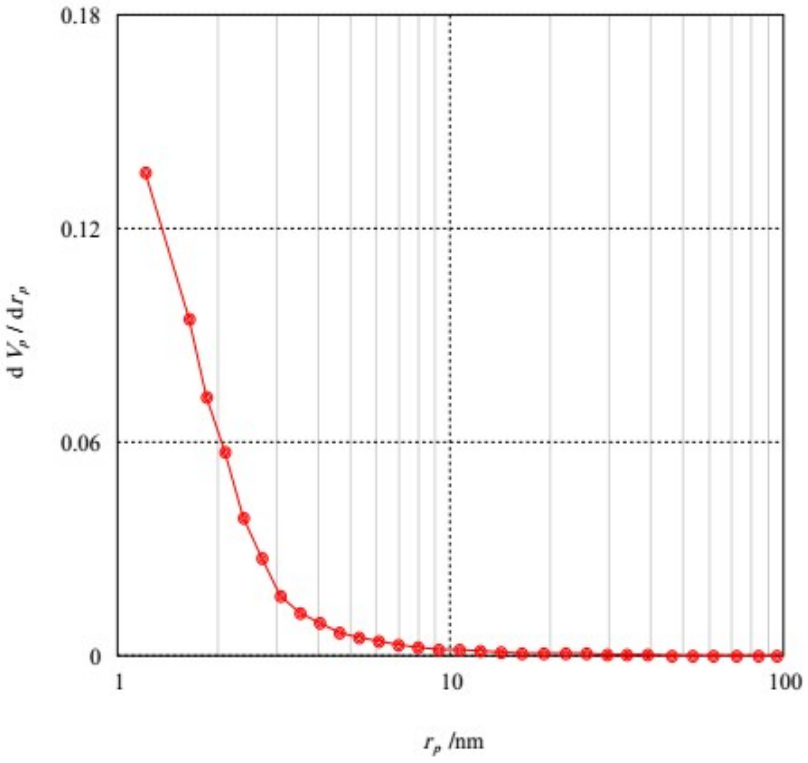

Figure S6. BJH pore size distributions analysis for NMCI-1 [D_{BJH} = 2.42 nm]

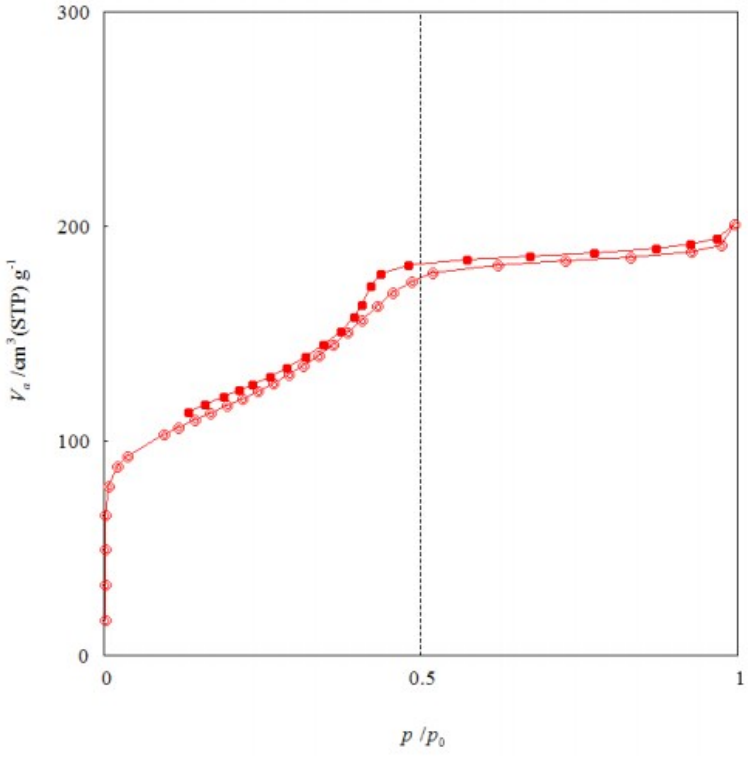

Figure S7. N_2 adsorption-desorption isotherm of CMK-3 [S_{BET} = 1005 m^2 g^{-1} and V_t = 1.31 cm^3 g^{-1}]

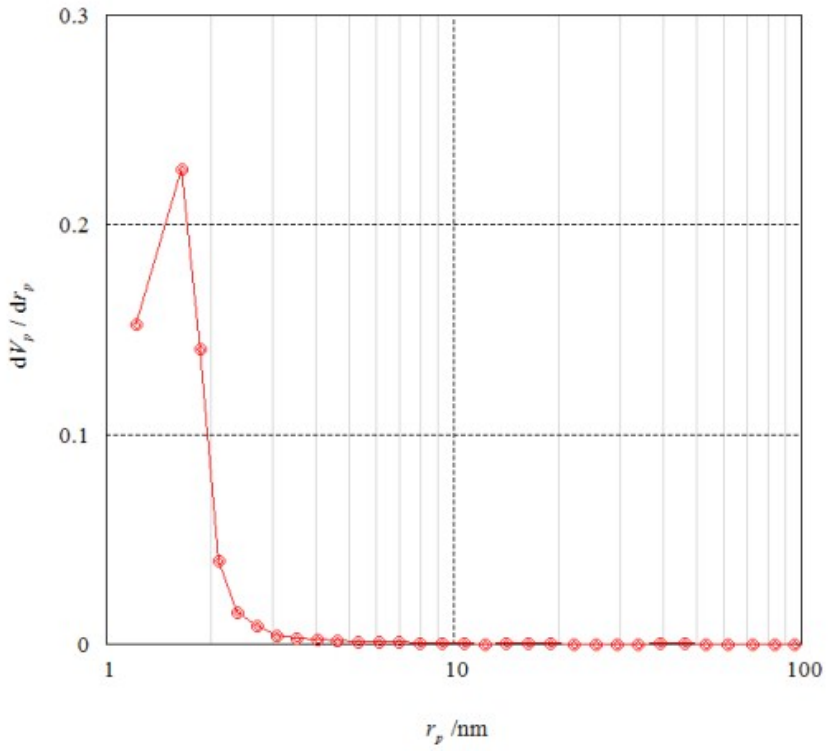

Figure S8. BJH pore size distributions analysis for CMK-3 [D_{BJH} = 3.28 nm]

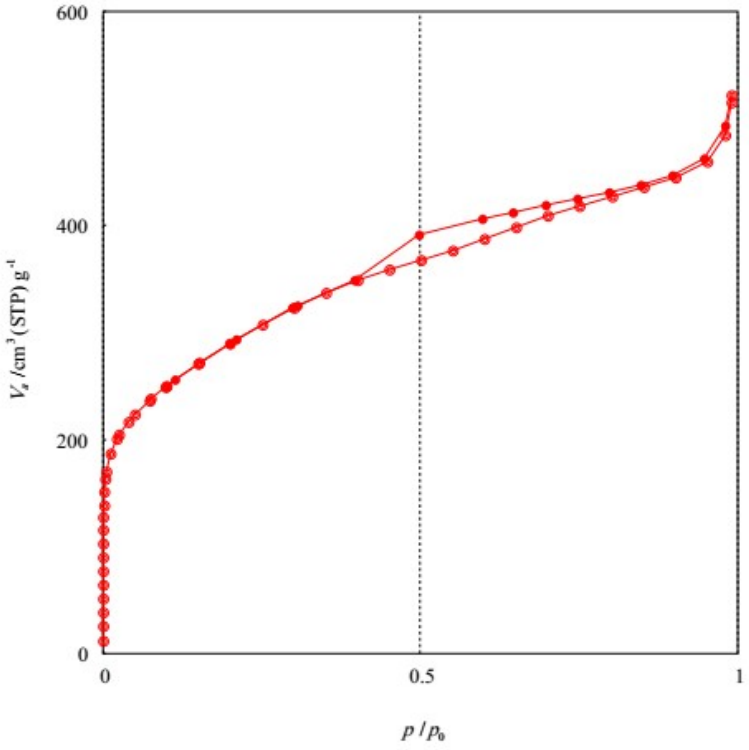

Figure S9. N_2 adsorption-desorption isotherm of NMCI-2 [S_{BET}=1026 m^2 g^{-1}, V_t = 0.8 cm^3 g^{-1}]

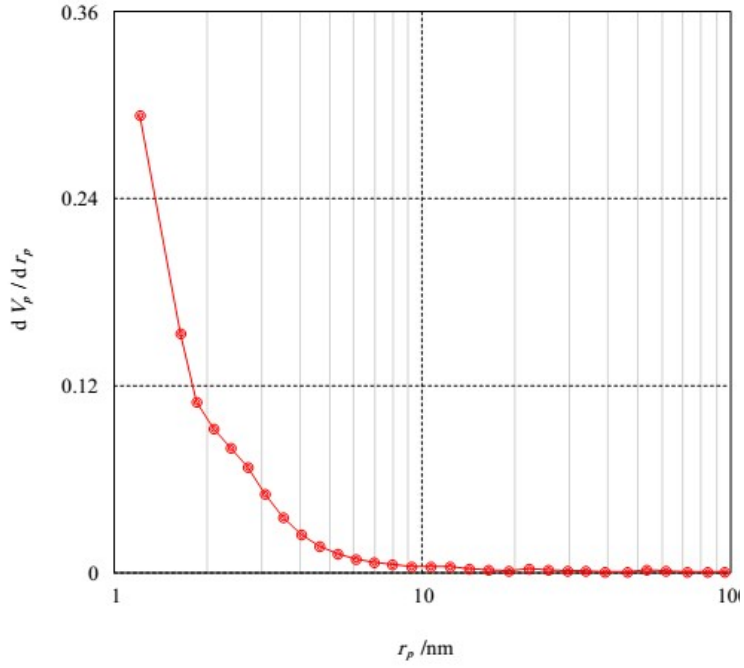

Figure S10. BJH pore size distribution analysis of NMCI-2 [D_{BJH} = 2.42 nm]

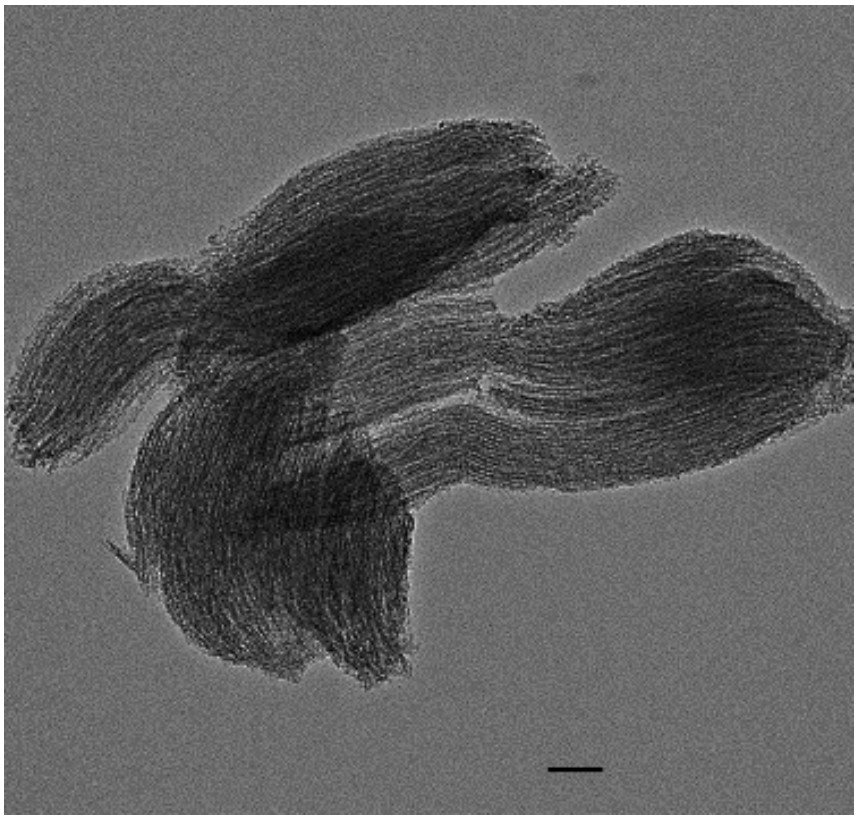

Figure S11. TEM image of NMCI-2 (Scale bar:100 nm)

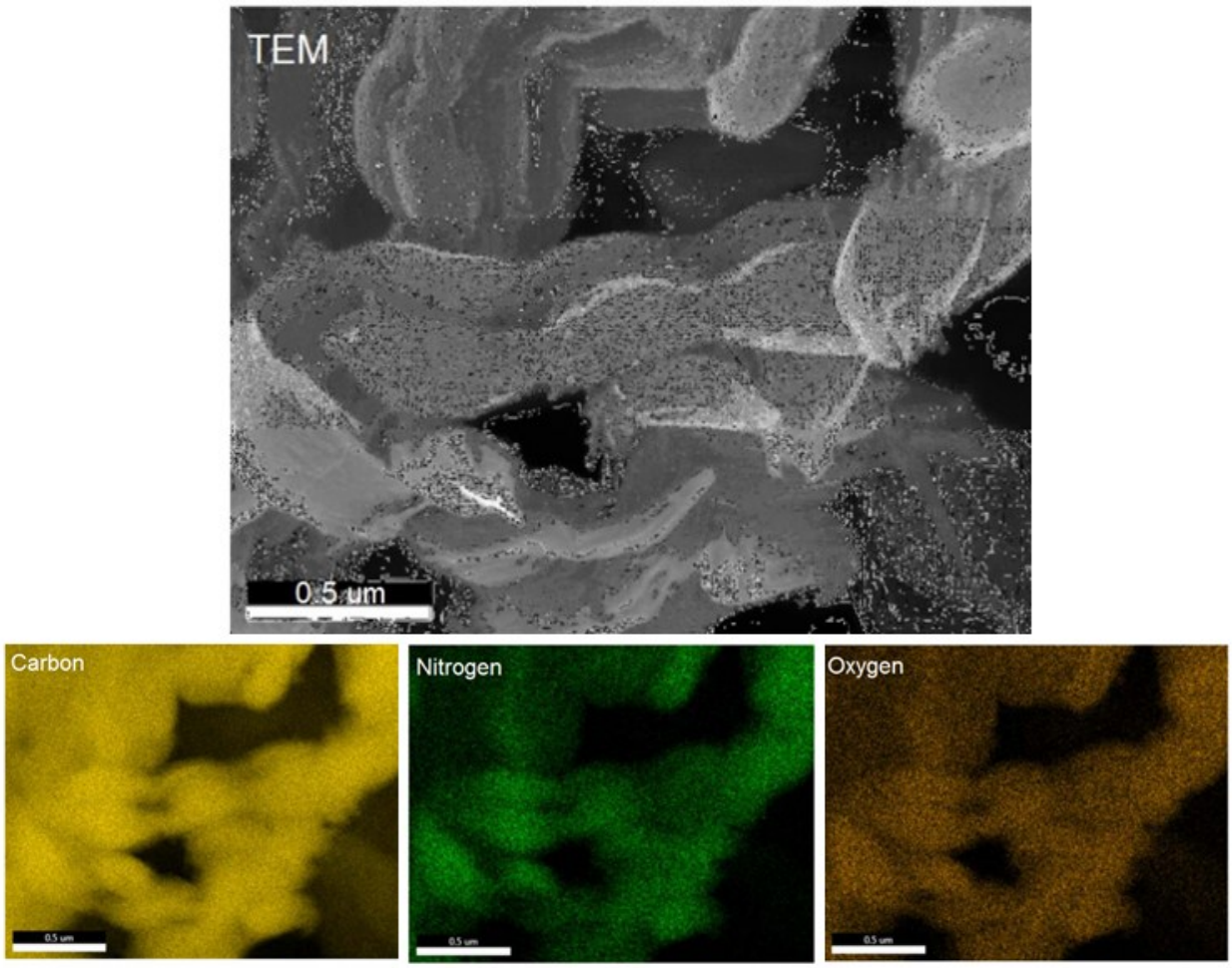

Figure S12. Qualitative elemental mapping NMCI-2 (The scale bar is 5µm)

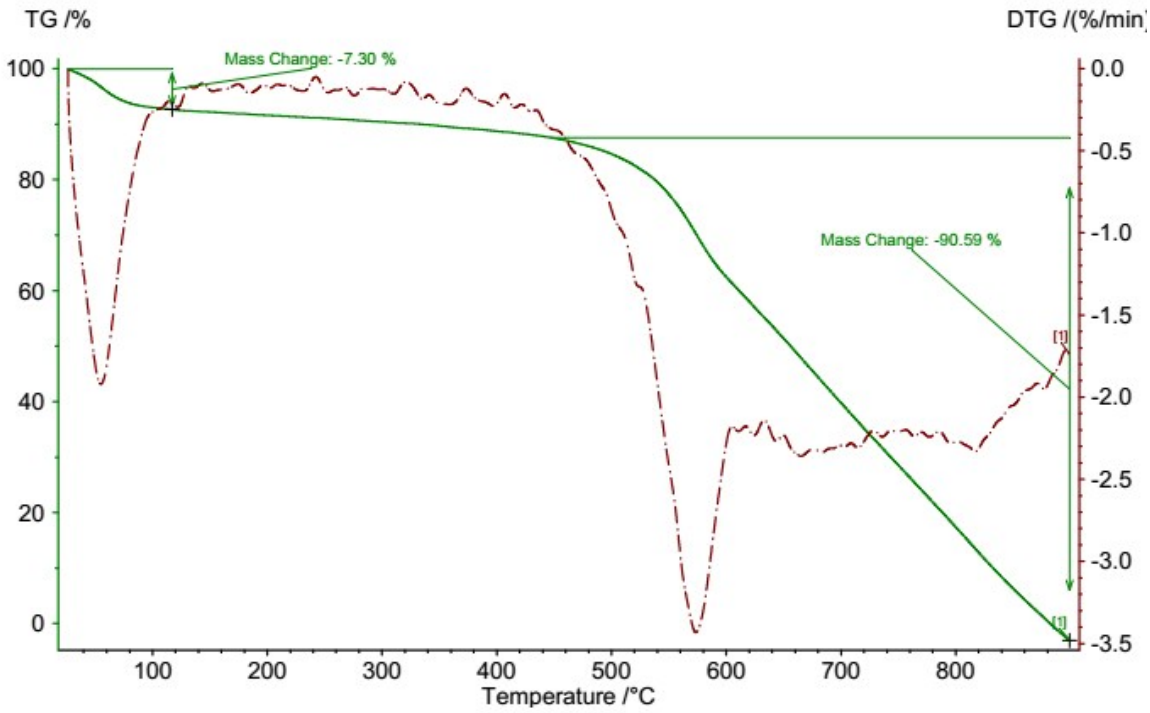

Figure S13. TGA pattern for NMCI-2

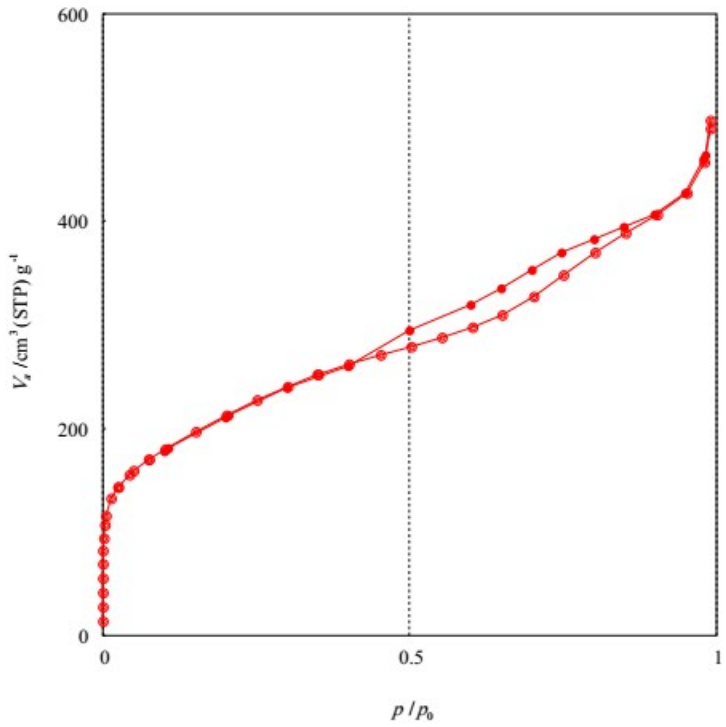

Figure S14. N_2 adsorption-desorption isotherm of Au-Pd@NMCI-2 [S_{BET}=750 m^2 g^{-1}, V_t=0.70 cm^3 g^{-1}]

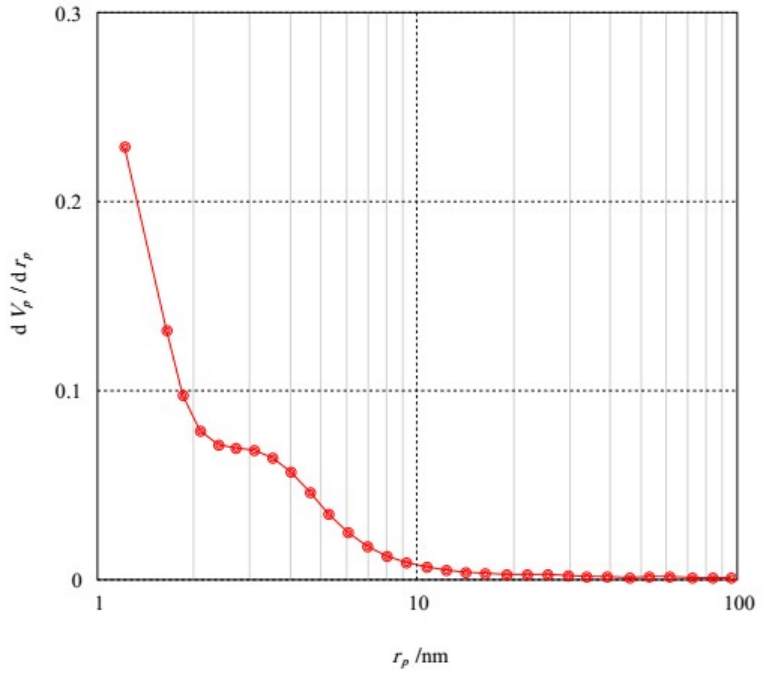

Figure S15. BJH pore size distribution analysis of Au-Pd@NMCI-2

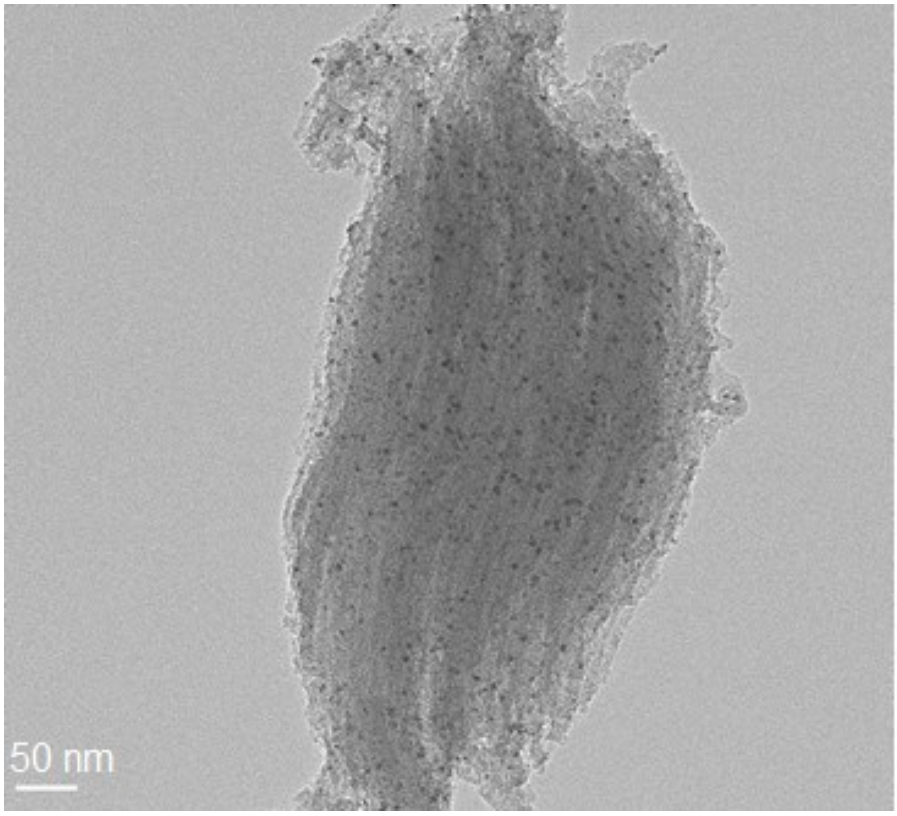

Figure S16. TEM image of Au-Pd@NMCI-2

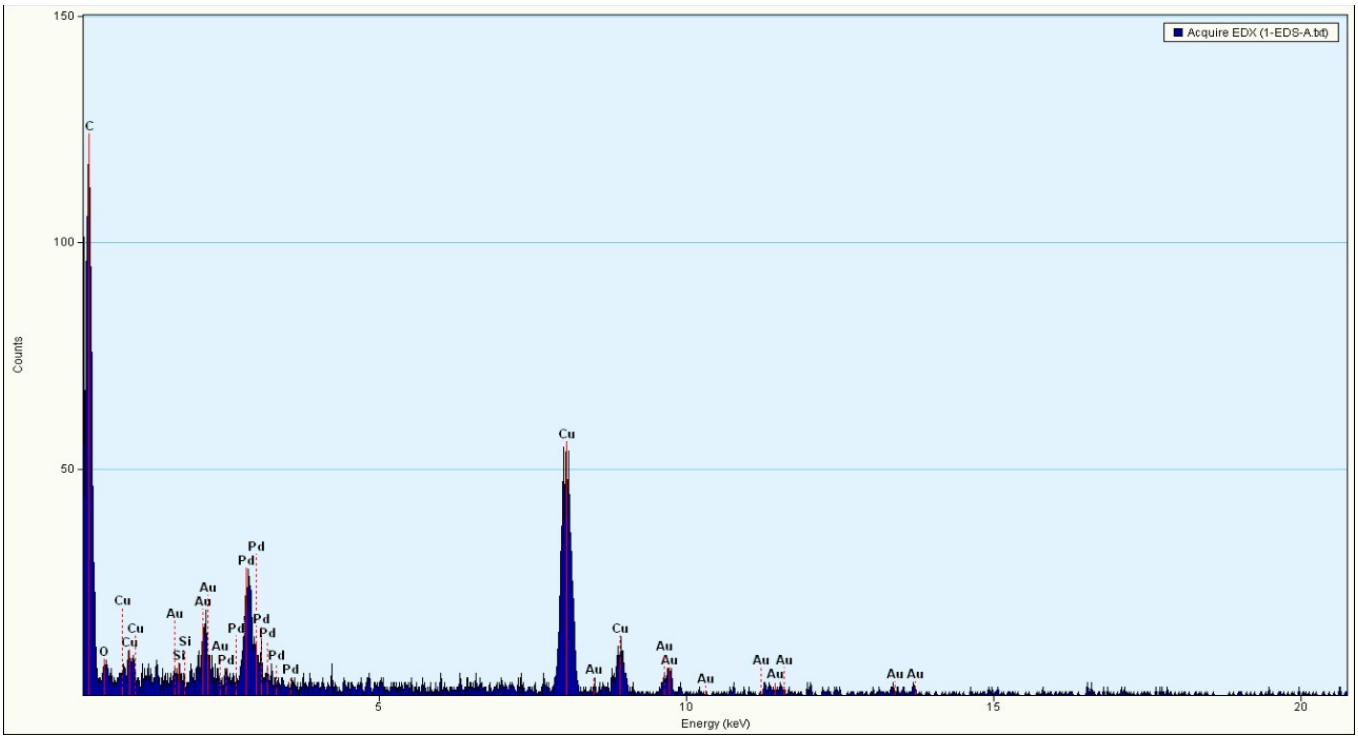

Figure S17. EDX spectra for Au-Pd@NMCI-2

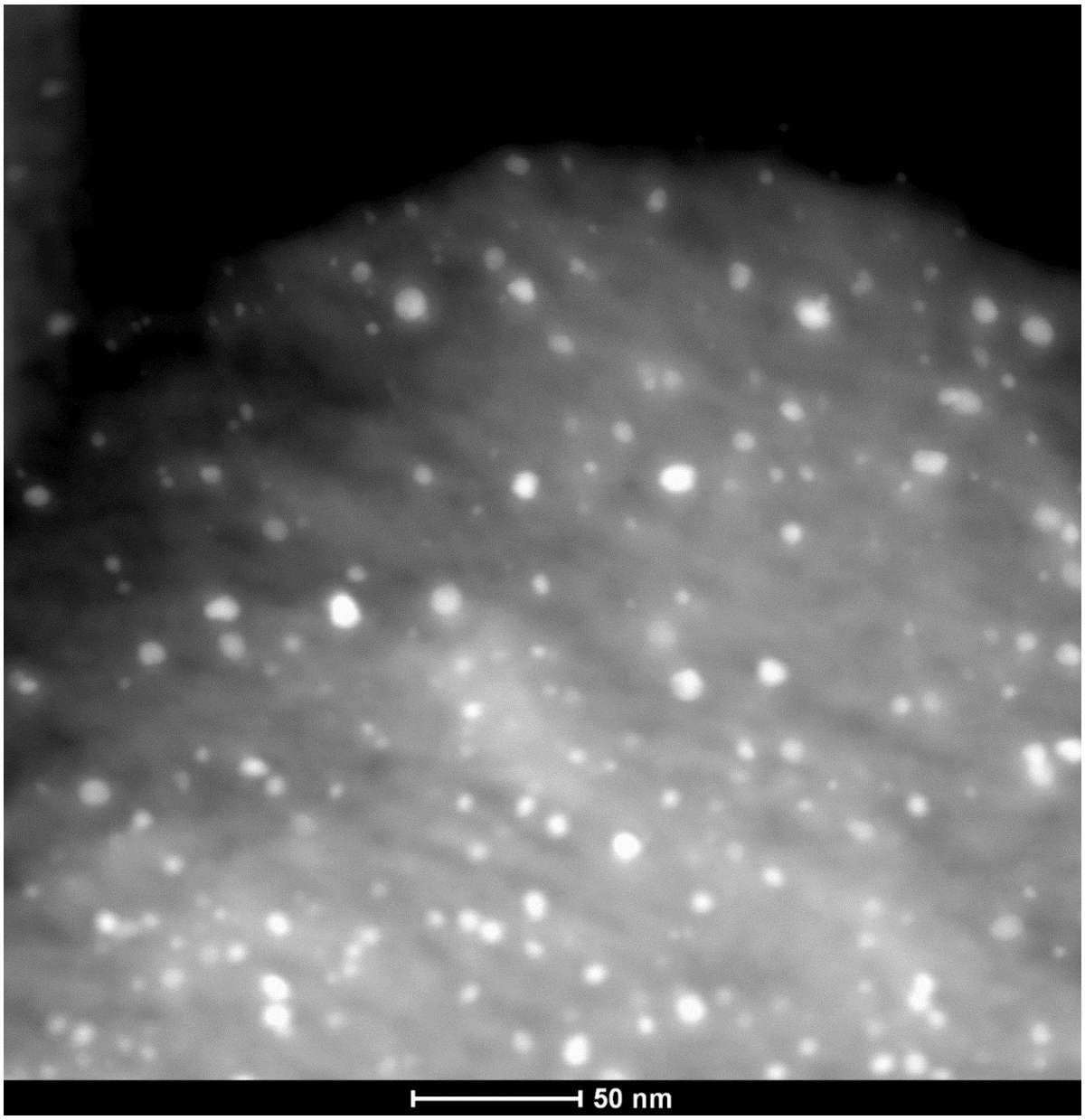

Figure S18. High angle annular dark field (HAADF) image of the Au-Pd@NMCI-2

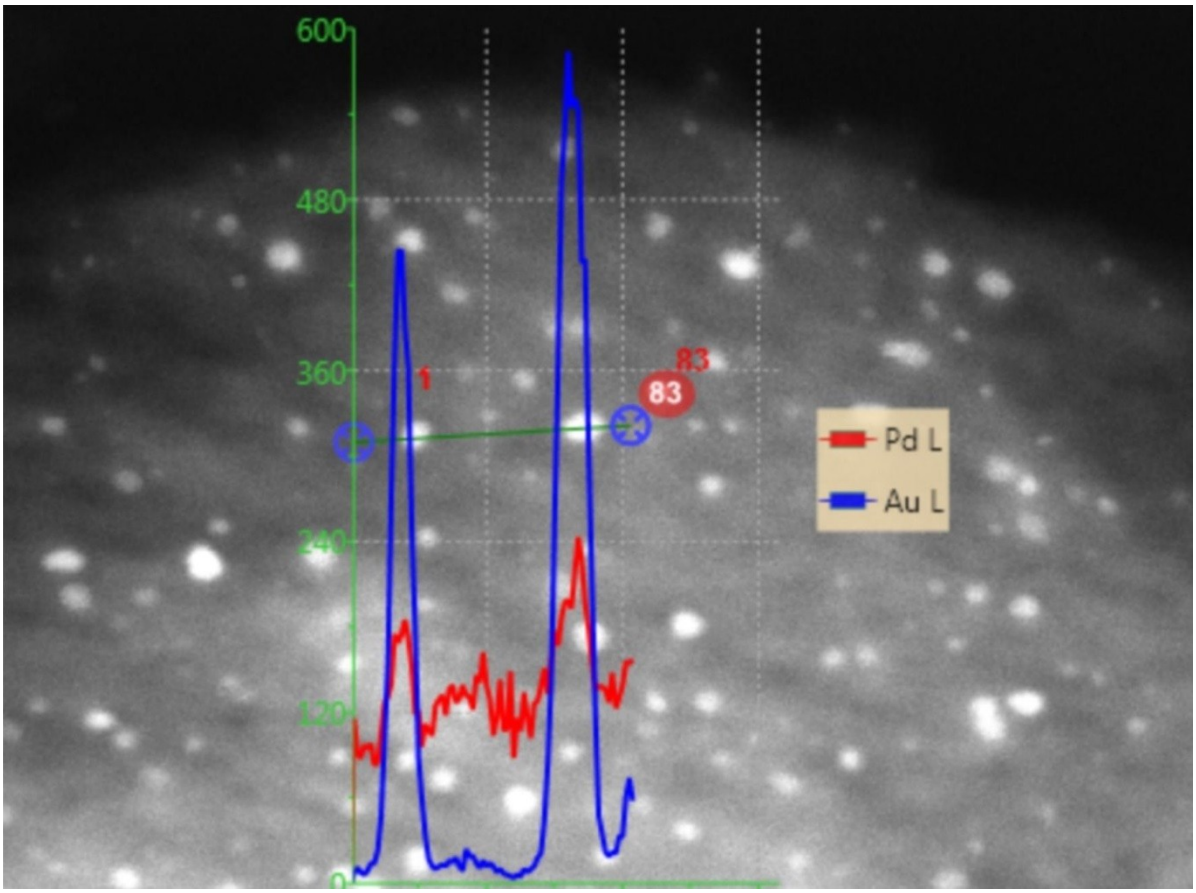

Figure S19. Element profile plot of Au-Pd@NMCI-2

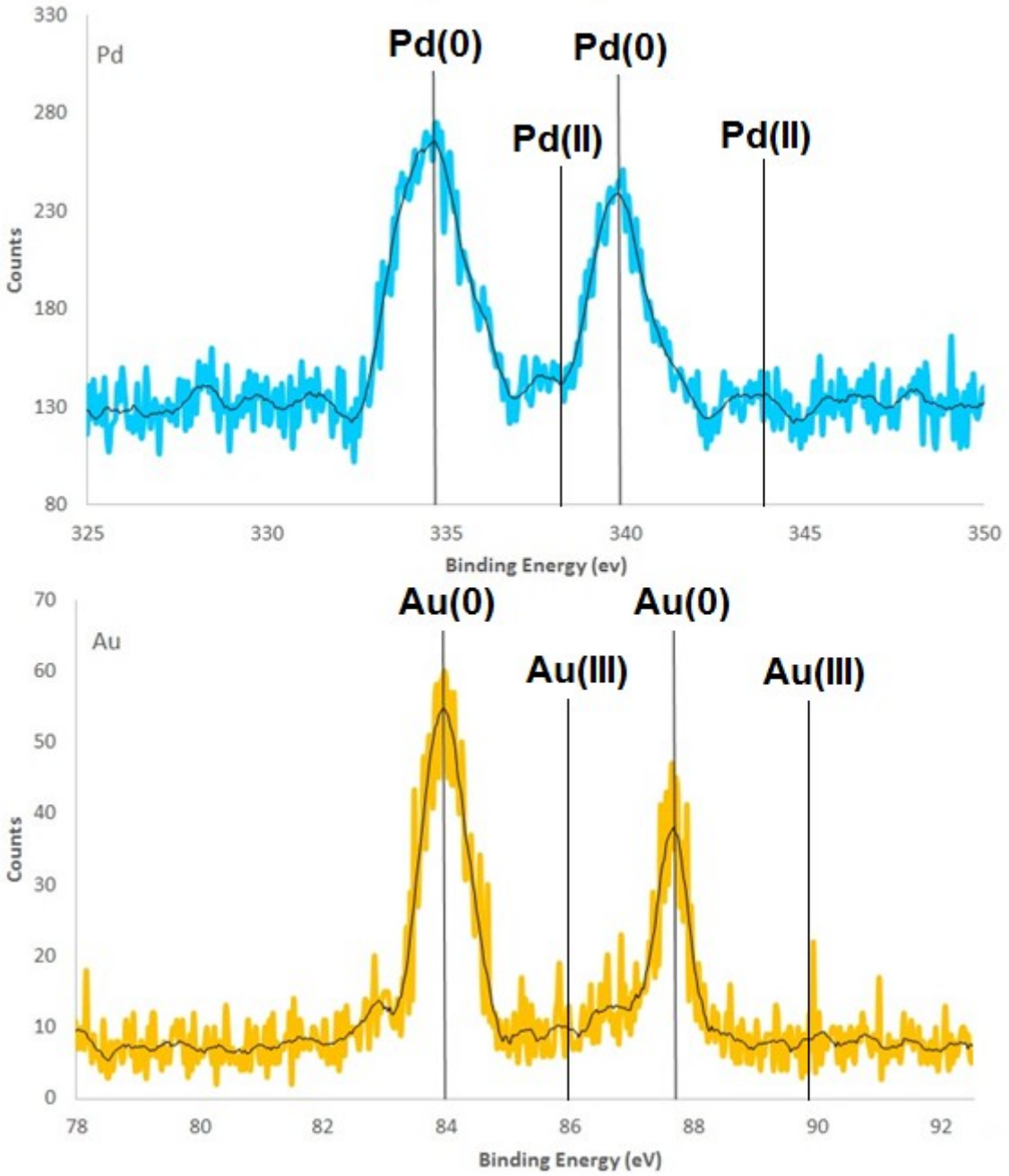

Figure S20. The XPS spectrums of the Au-Pd@NMCI-2 [Pd (up) and Au (down)]

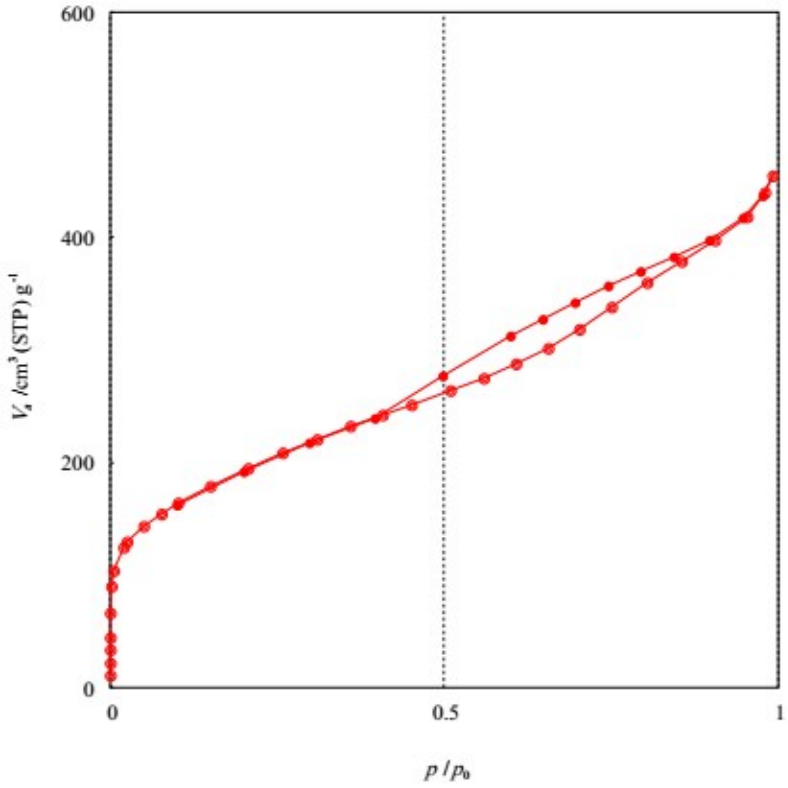

Figure S21. N_2 adsorption-desorption isotherm of the recycled Au-Pd@NMCI-2. [S_{BET}=692 m^2 g^{-1} and V_t = 0.698 cm^3 g^{-1}]

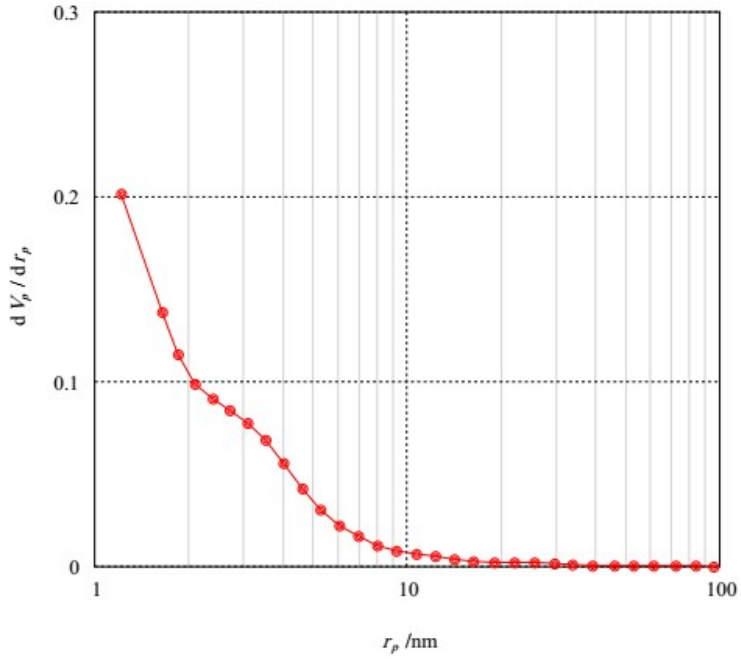

Figure S22. BJH pore size distribution analysis of the recycled Au-Pd@NMCI-2

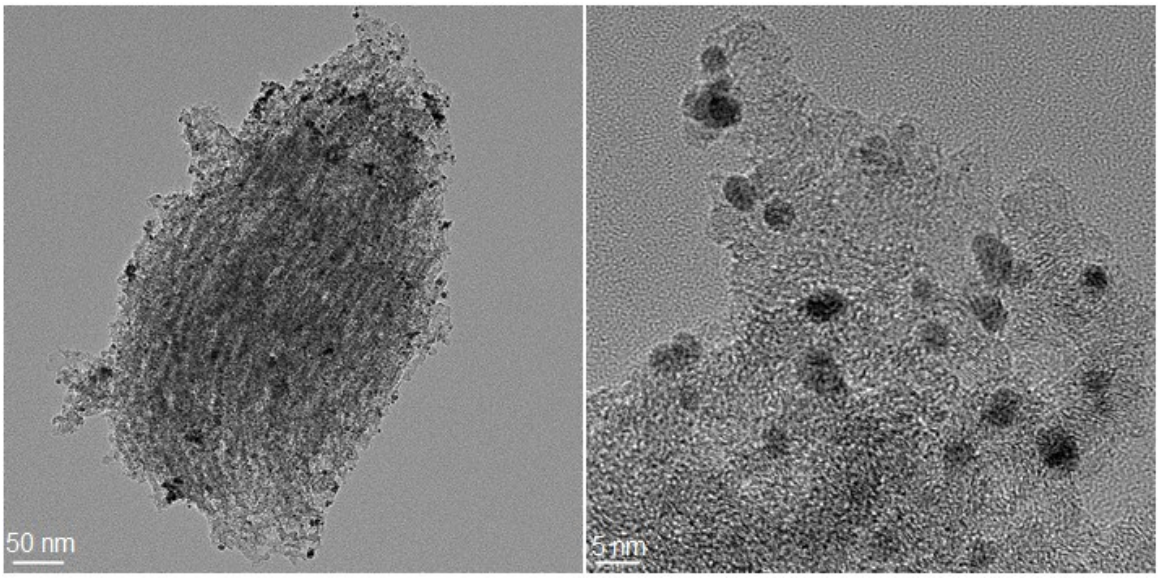

Figure S23. TEM image of the recycled Au-Pd@NMCI-2

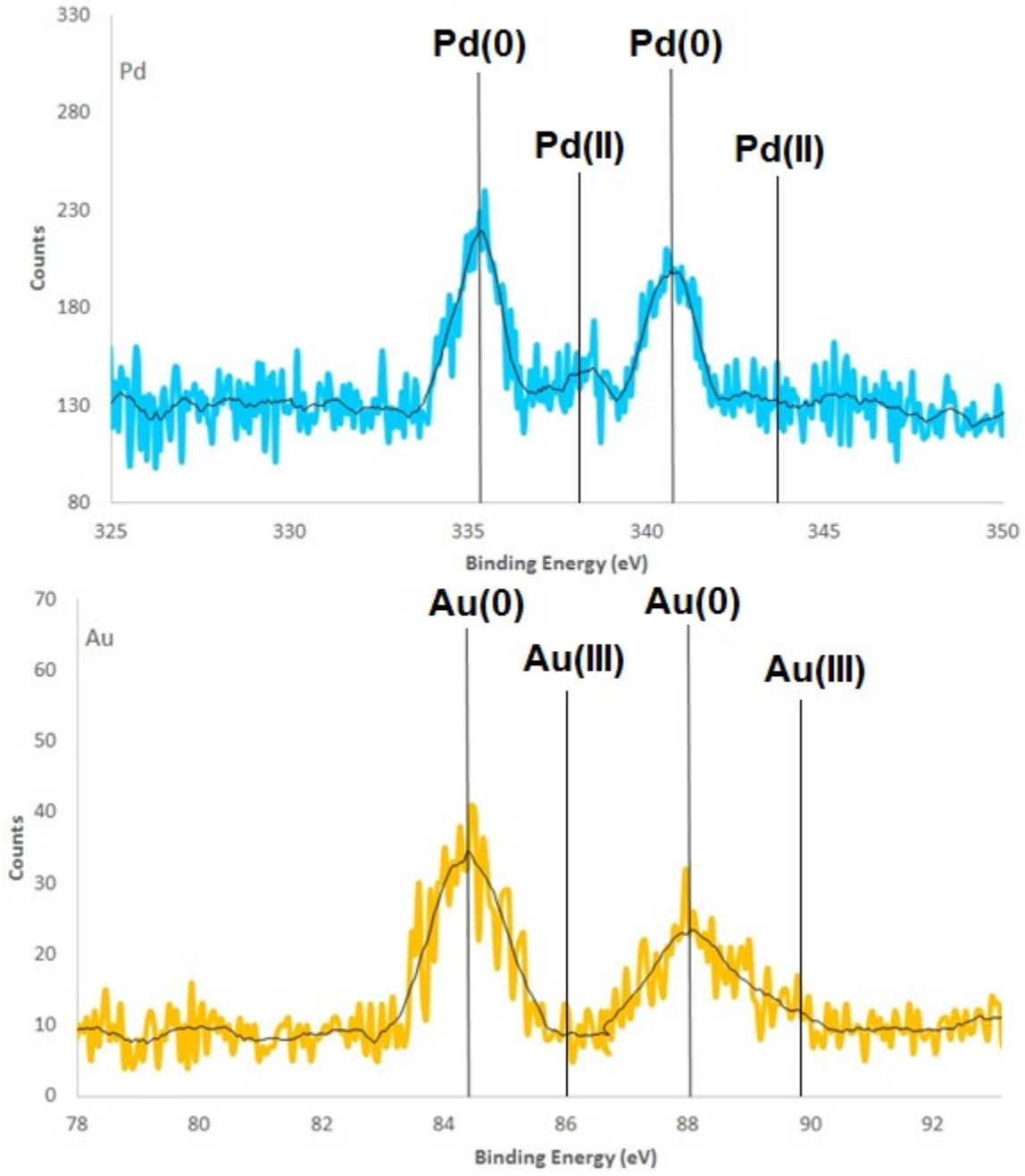

Figure S24. The XPS spectrums of the recycled Au-Pd@NMCI-2 [Pd (up) and Au (down)]

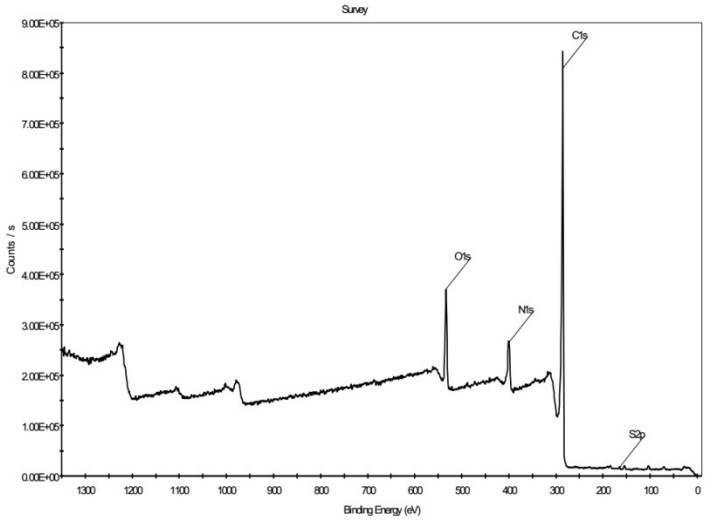

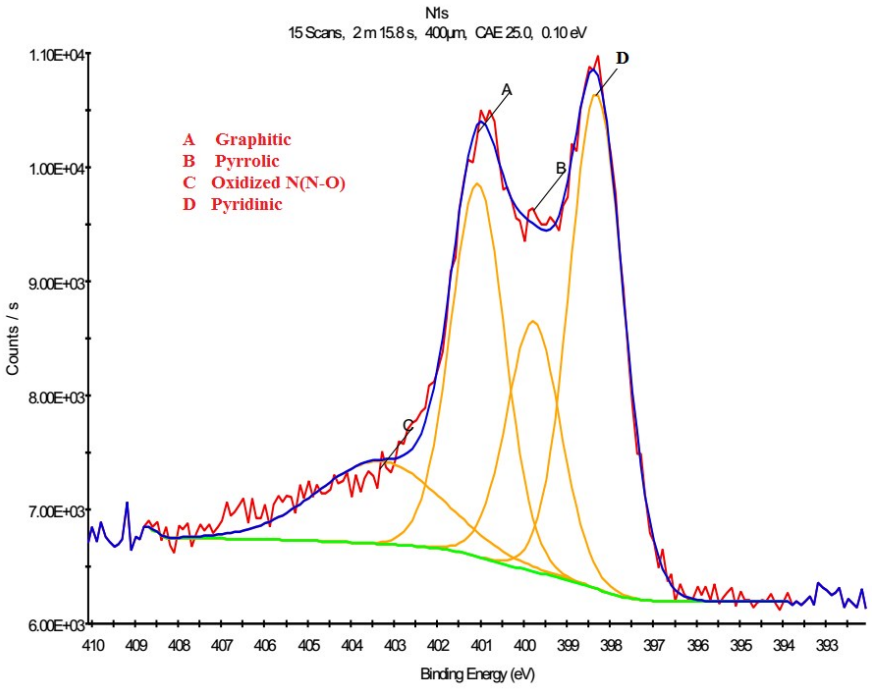

Elemental ID and Quantification

Name	Peak BE	FWHM eV	Area (P) CPS.eV	Atomic %	Q	SF
D	398.31	1.48	6944.26	37.82	1	1.676
A	401.06	1.48	5242.77	28.61	1	1.676
B	399.77	1.48	3504.68	19.11	1	1.676
C	403.33	3.37	2647.10	14.47	1	1.676

Figure S25. The XPS spectrums of NMCI-2 [Full survey (up) and N1s region (down)]

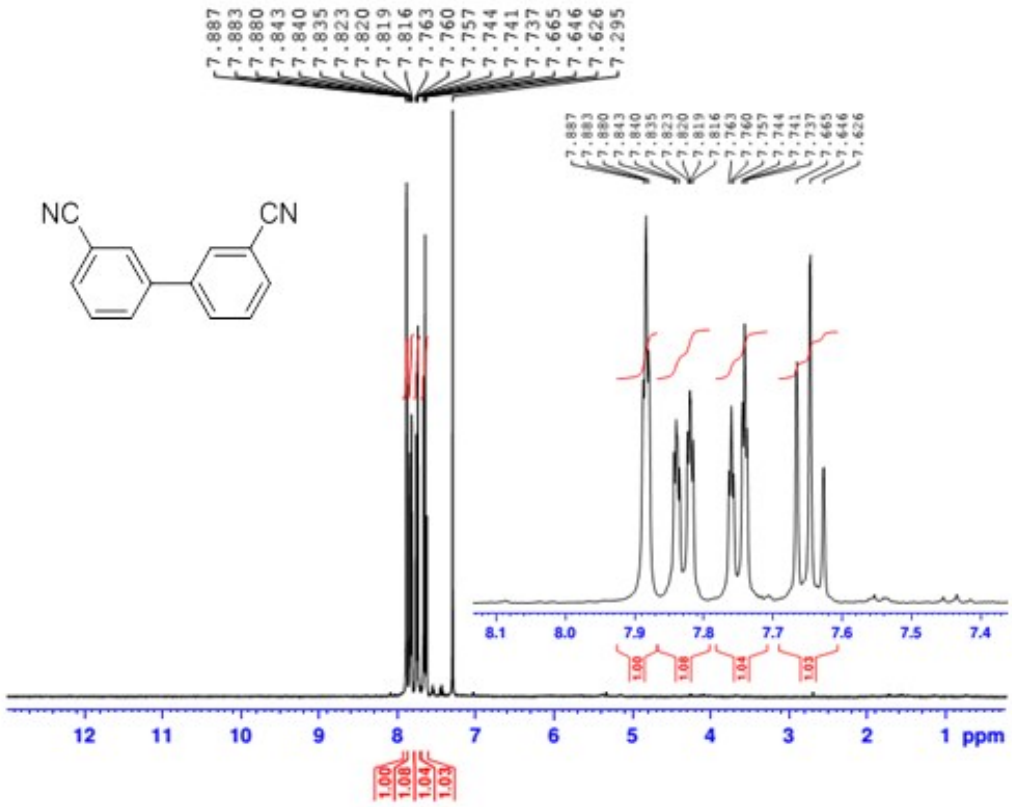

Figure S26. ^{1}H-NMR spectrum (400 MHz, $CDCl_3$) of [1,1'-biphenyl]-3,3'-dicarbonitrile

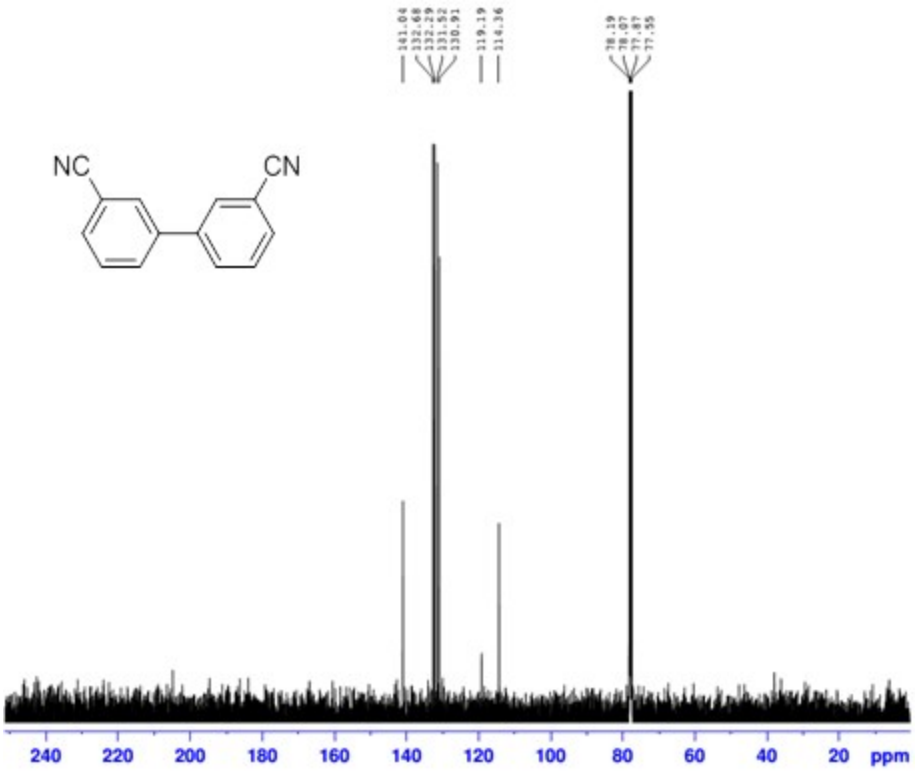

Figure S27. ^{13}C-NMR spectrum (100 MHz, $CDCl_3$) of [1,1'-biphenyl]-3,3'-dicarbonitrile

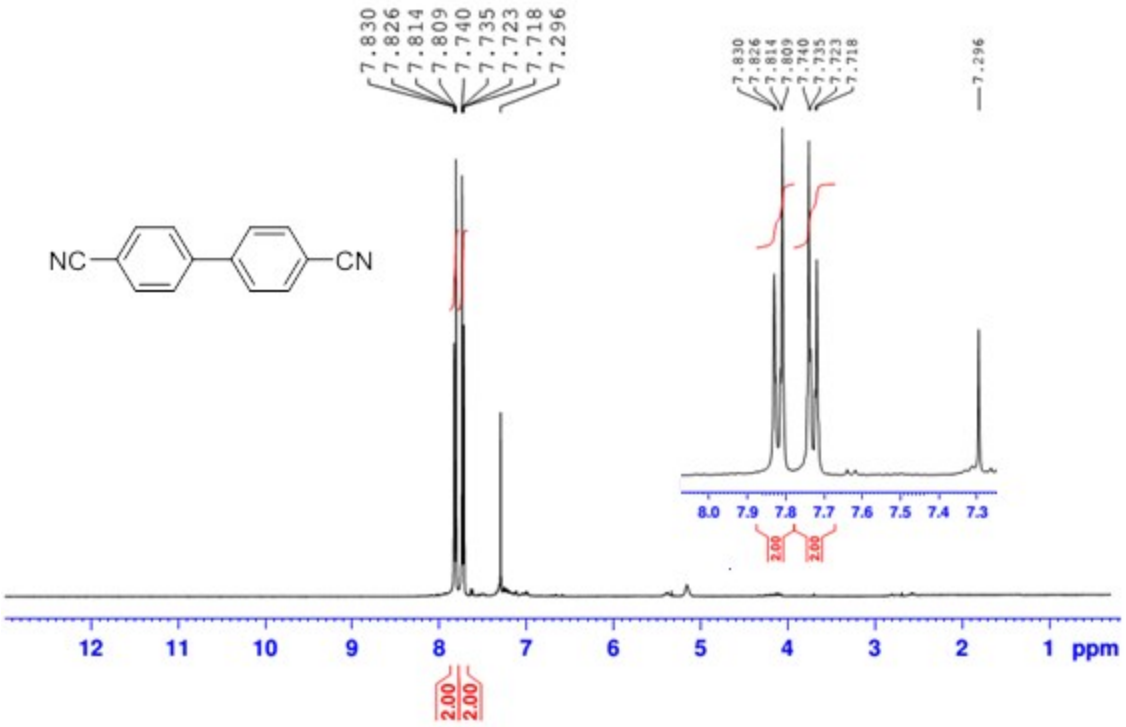

Figure S28. ^{1}H-NMR spectrum (400 MHz, $CDCl_3$) of [1,1'-biphenyl]-4,4'-dicarbonitrile

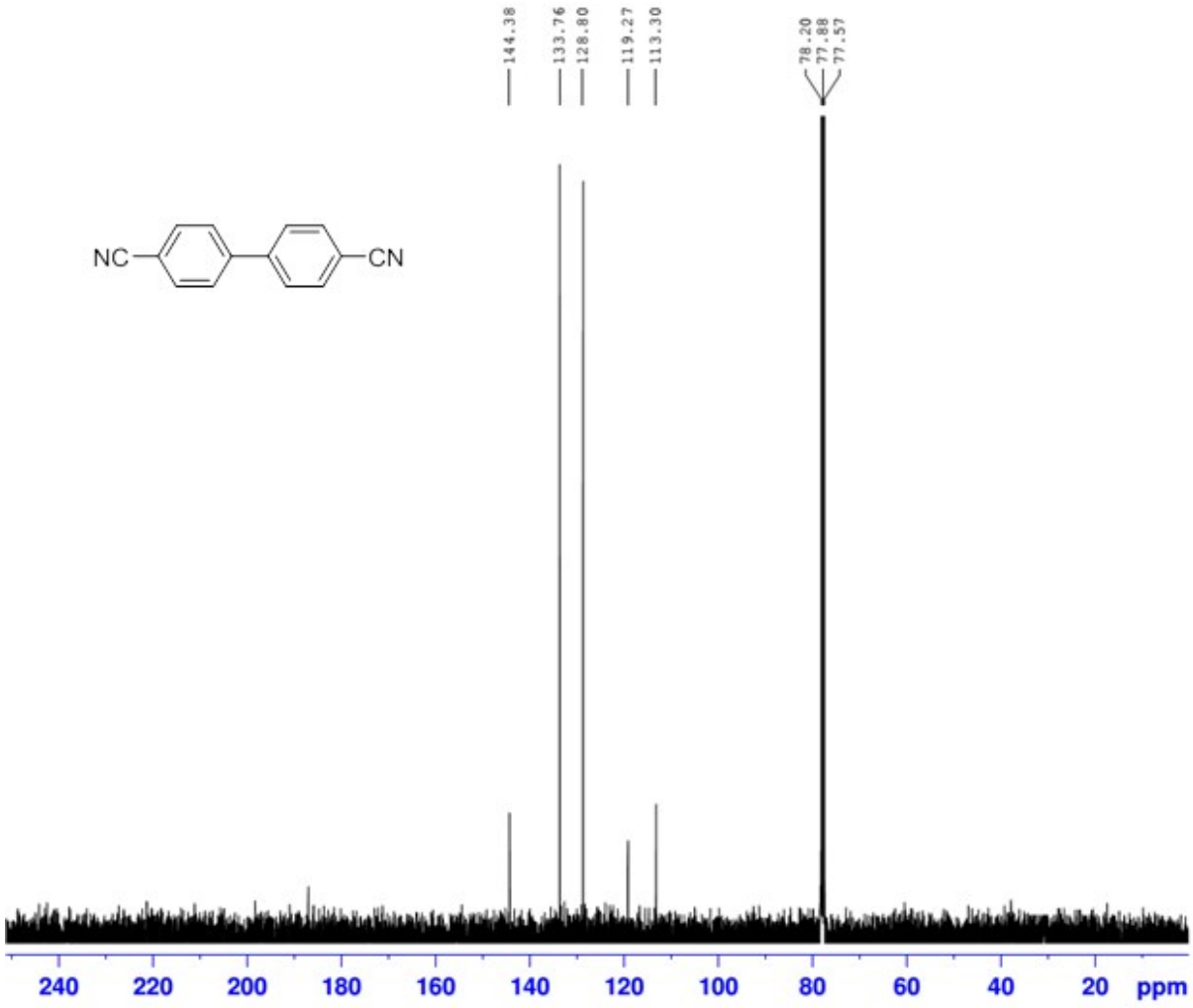

Figure S29. ^{13}C-NMR spectrum (100 MHz, $CDCl_3$) of [1,1'-biphenyl]-4,4'-dicarbonitrile

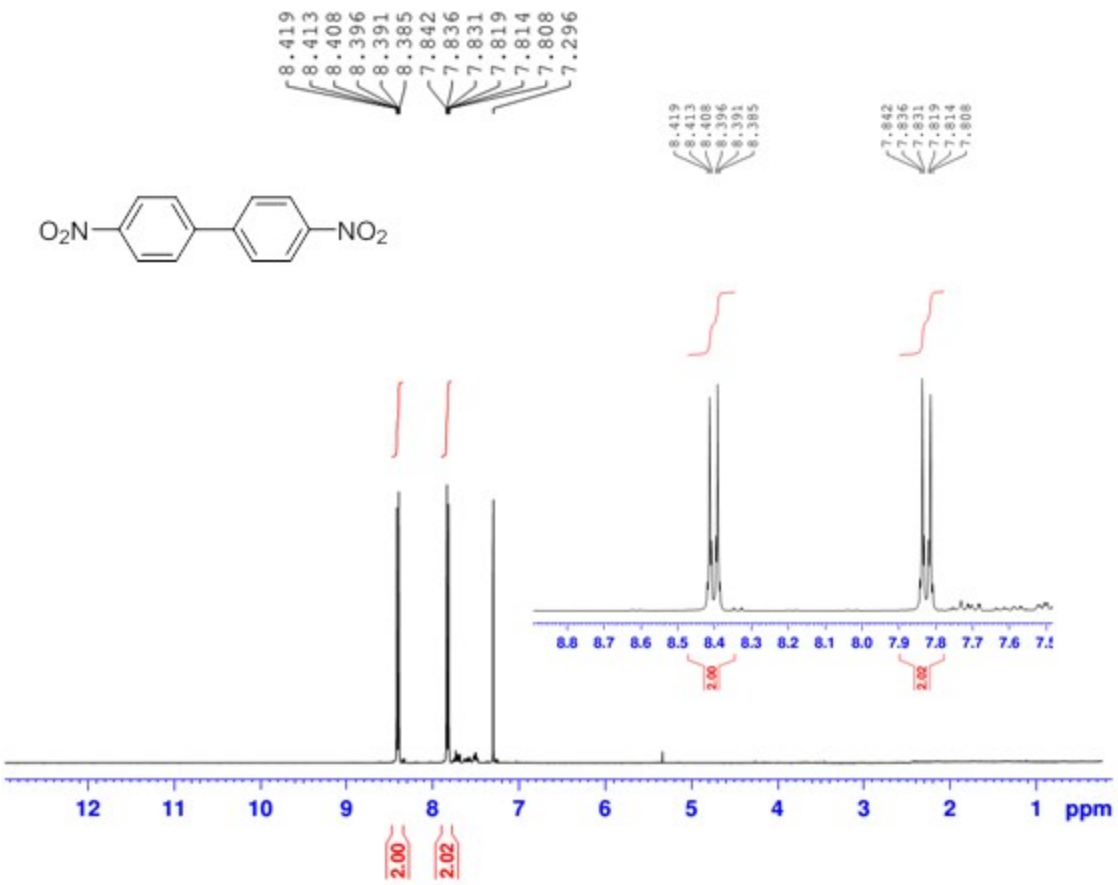

Figure S30. ^{1}H-NMR spectrum (400 MHz, $CDCl_3$) of 4,4'-dinitro-1,1'-biphenyl

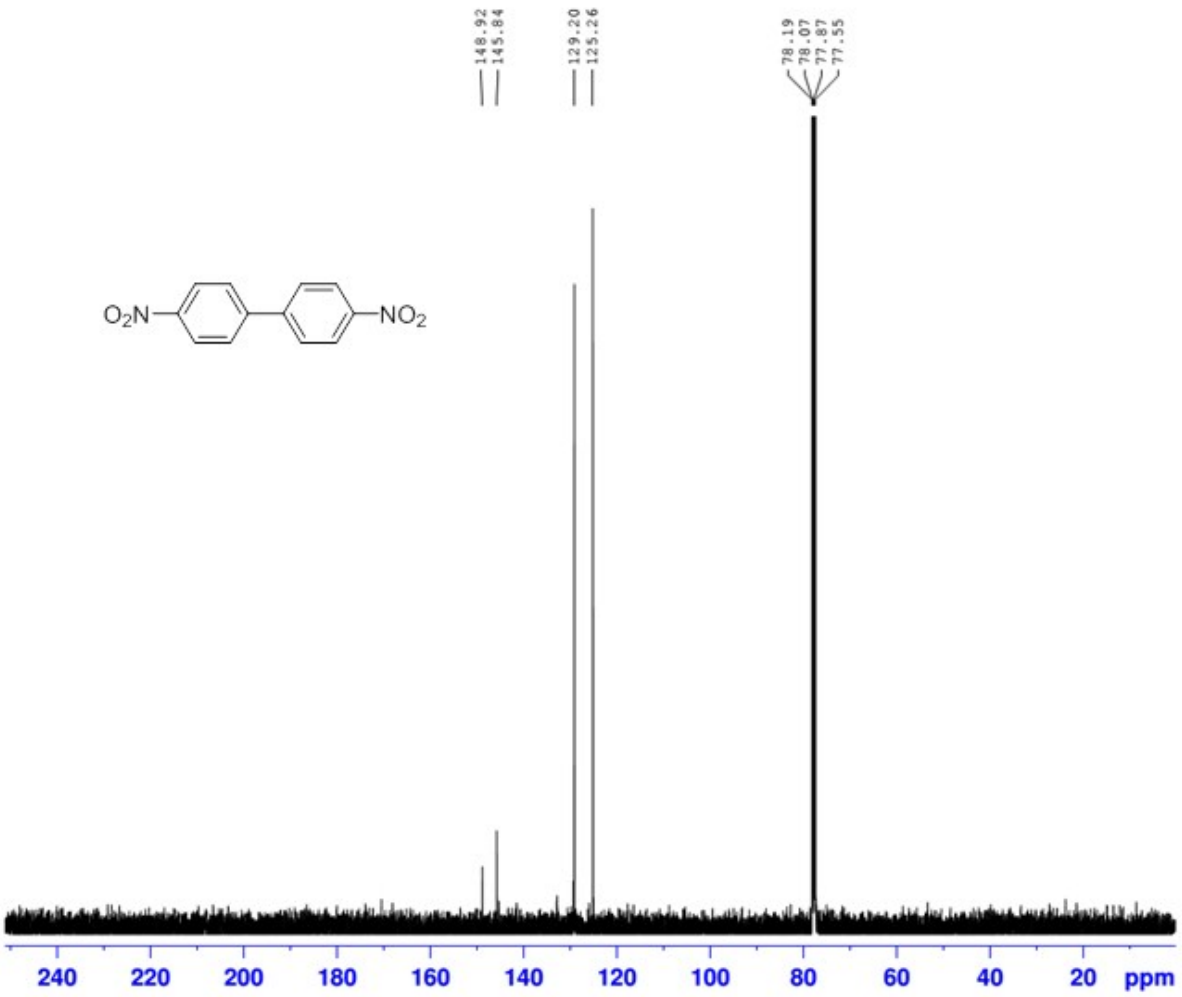

Figure S31. ^{13}C-NMR spectrum (100 MHz, $CDCl_3$) of 4,4'-dinitro-1,1'-biphenyl

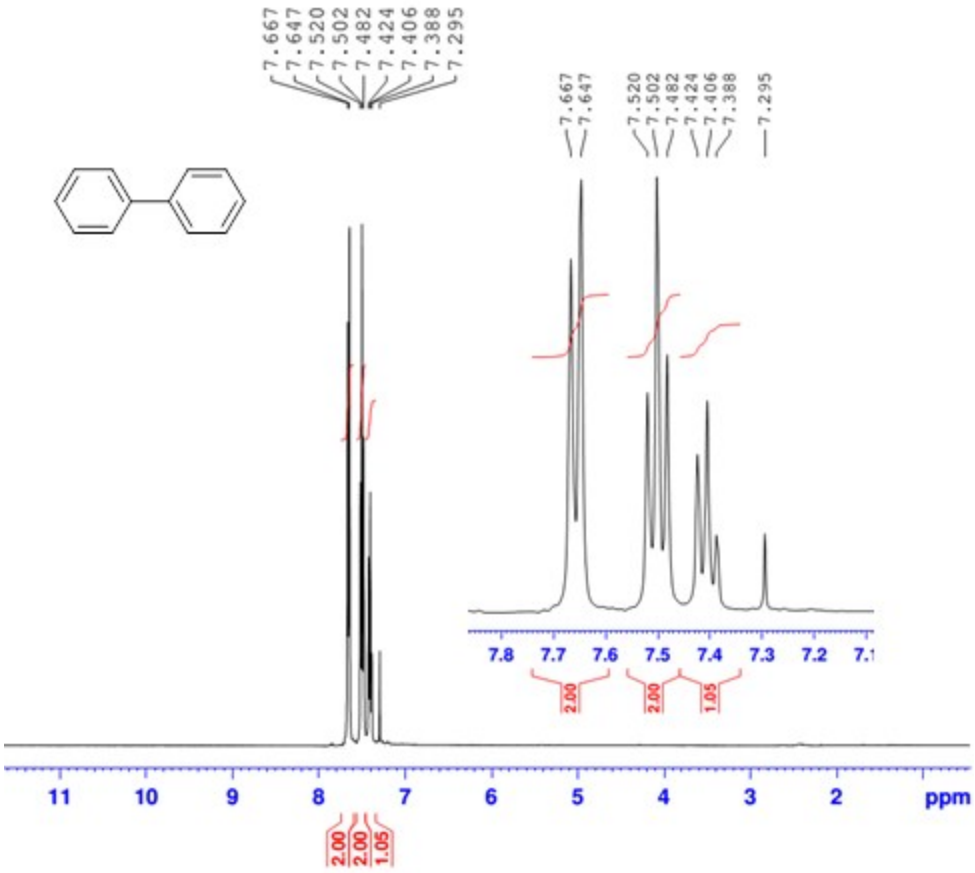

Figure S32. ^{1}H-NMR spectrum (400 MHz, $CDCl_3$) of 1,1'-biphenyl

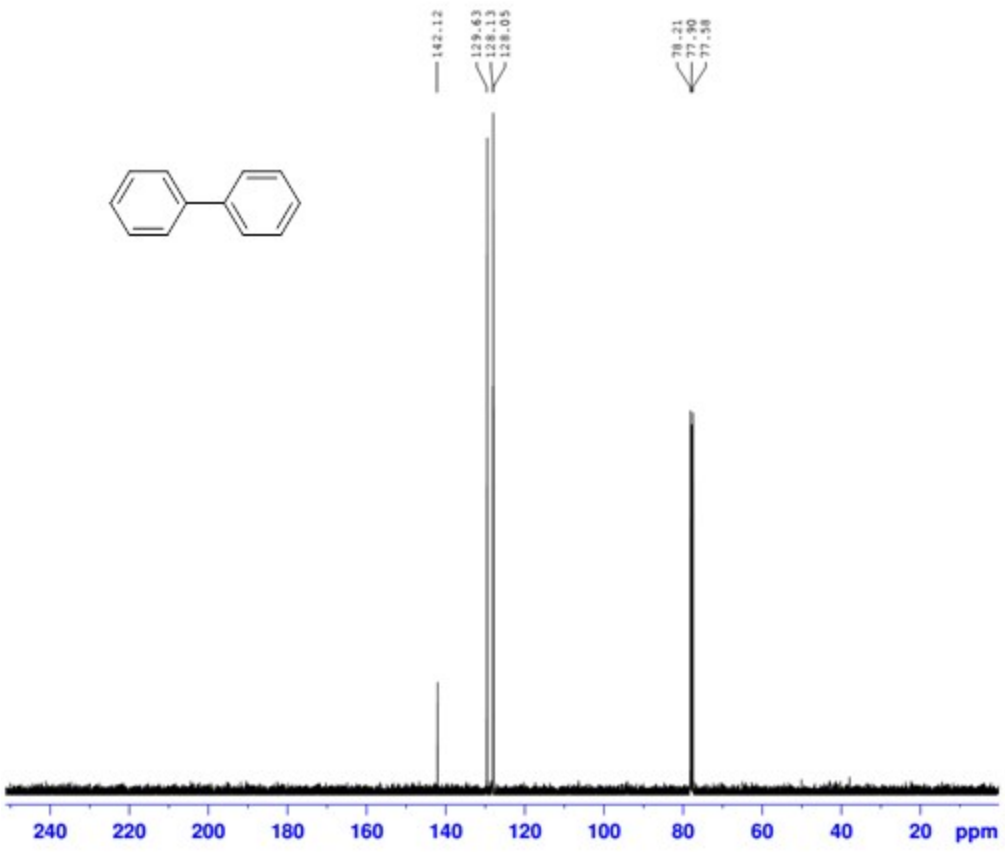

Figure S33. ^{13}C-NMR spectrum (100 MHz, $CDCl_3$) of 1,1'-biphenyl

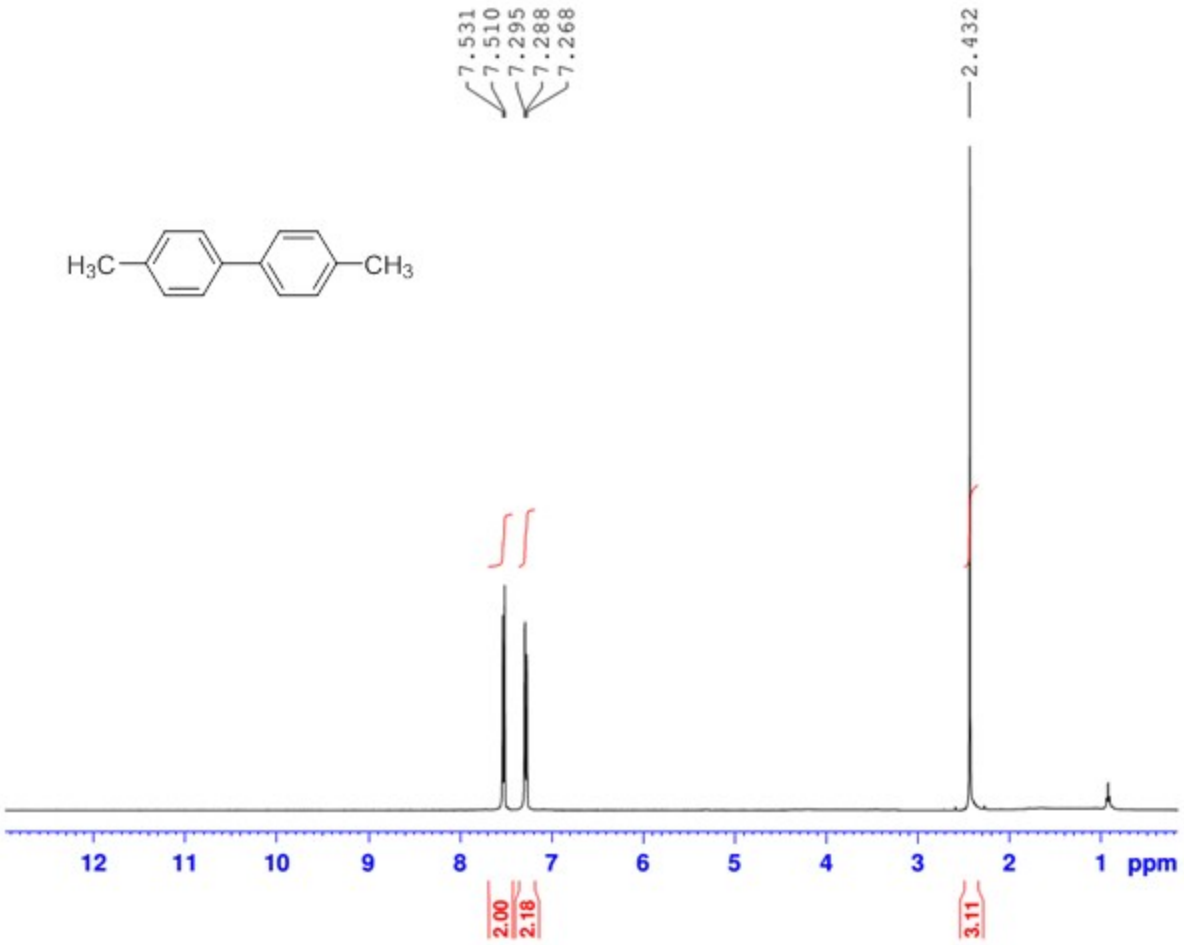

Figure S34. ^{1}H-NMR spectrum (400 MHz, $CDCl_3$) of 4,4'-dimethyl-1,1'-biphenyl

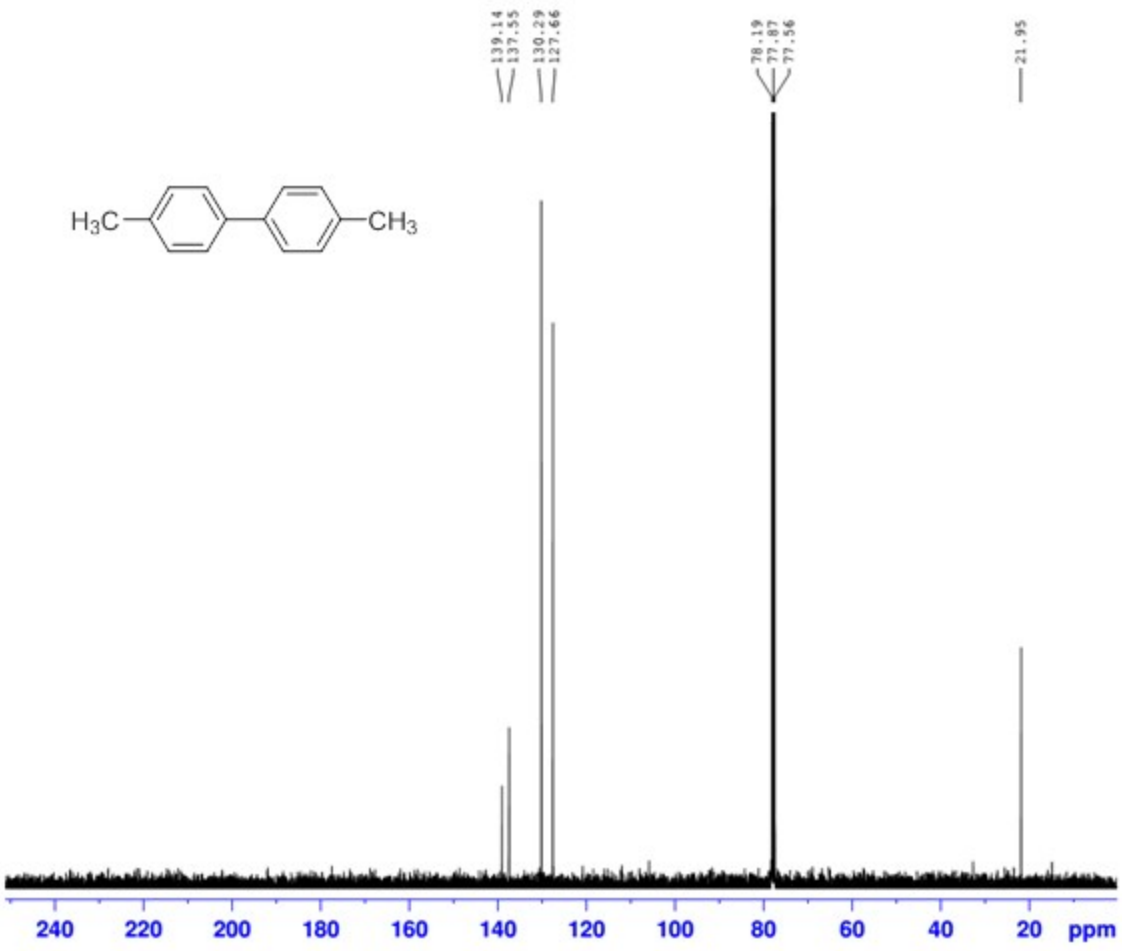

Figure S35. ^{13}C-NMR spectrum (100 MHz, $CDCl_3$) of 4,4'-dimethyl-1,1'-biphenyl

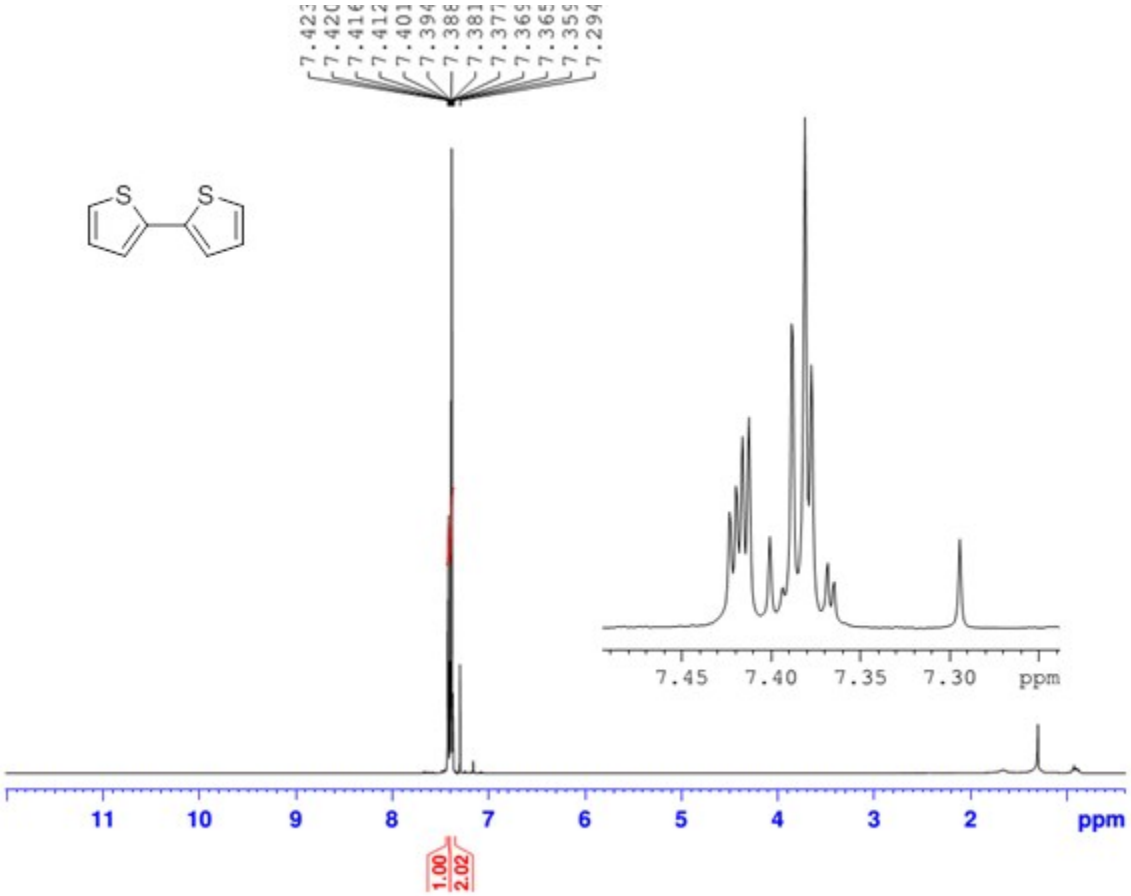

Figure S36. ^{1}H-NMR spectrum (400 MHz, $CDCl_3$) of 2,2'-bithiophene

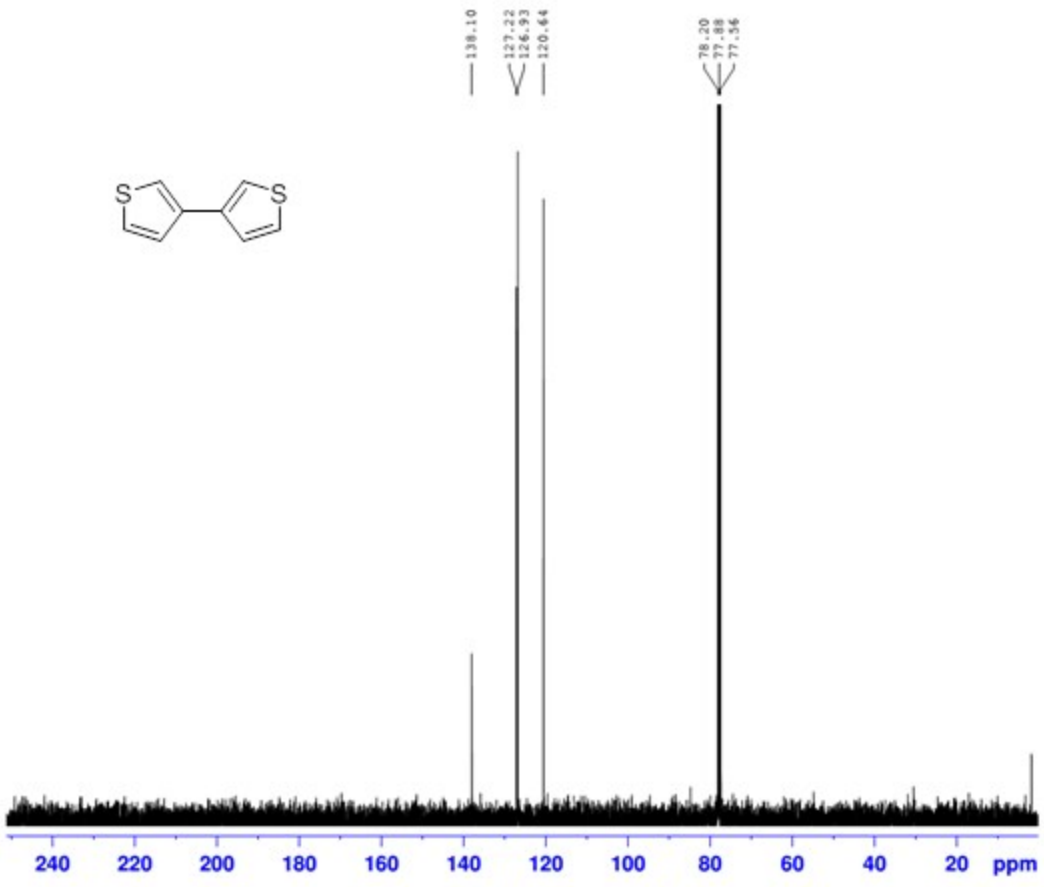

Figure S37. ^{13}C-NMR spectrum (100 MHz, $CDCl_3$) of 2,2'-bithiophene

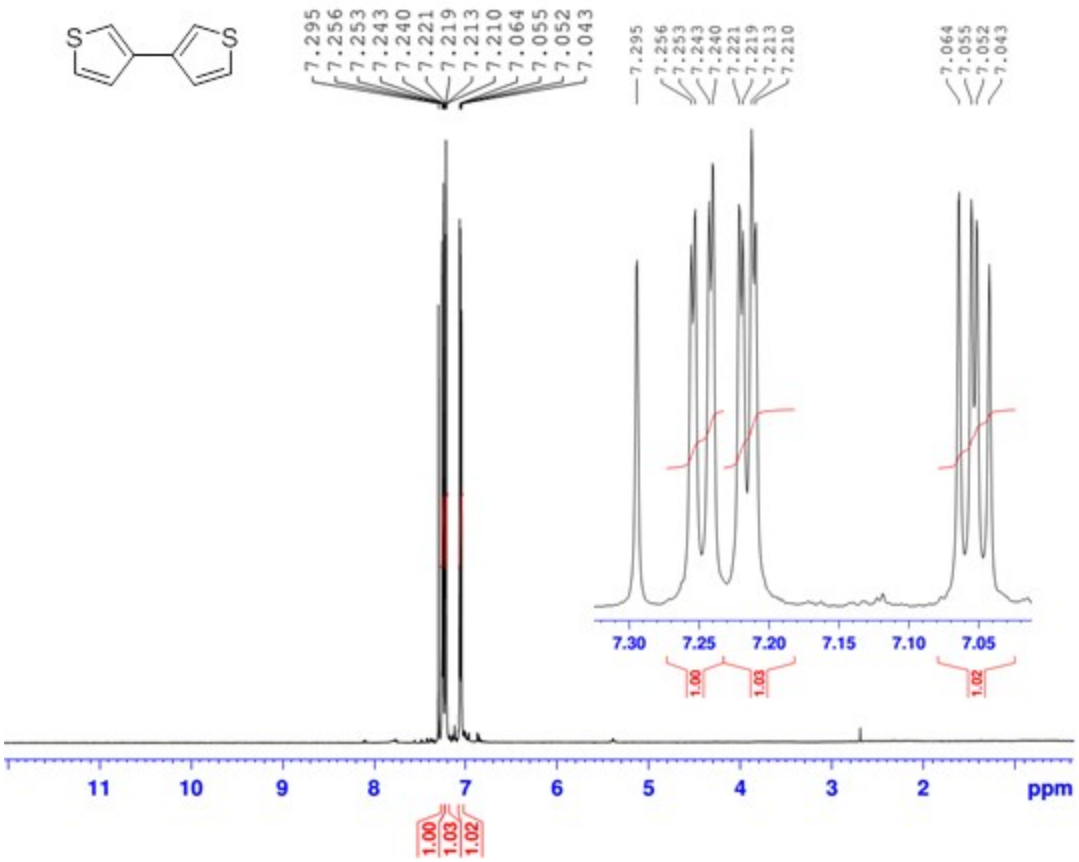

Figure S38. ^{1}H-NMR spectrum (400 MHz, $CDCl_3$) of 3,3'-bithiophene

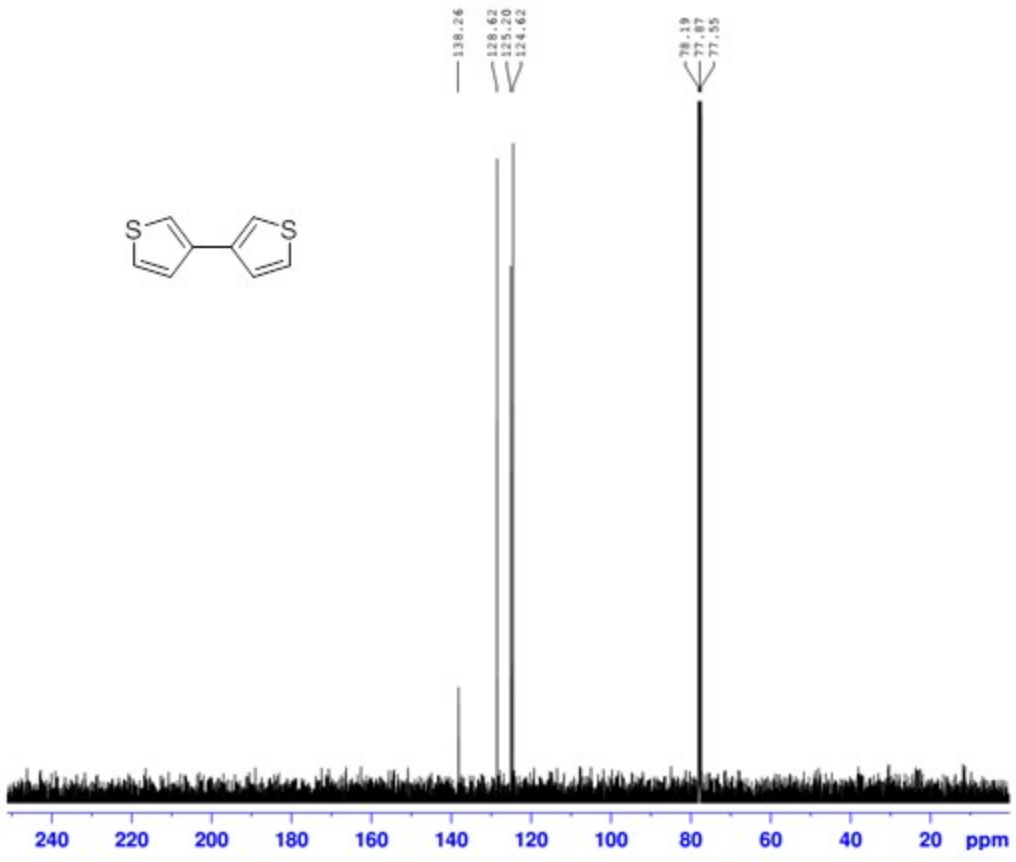

Figure S39. ^{13}C-NMR spectrum (100 MHz, $CDCl_3$) of 3,3'-bithiophene

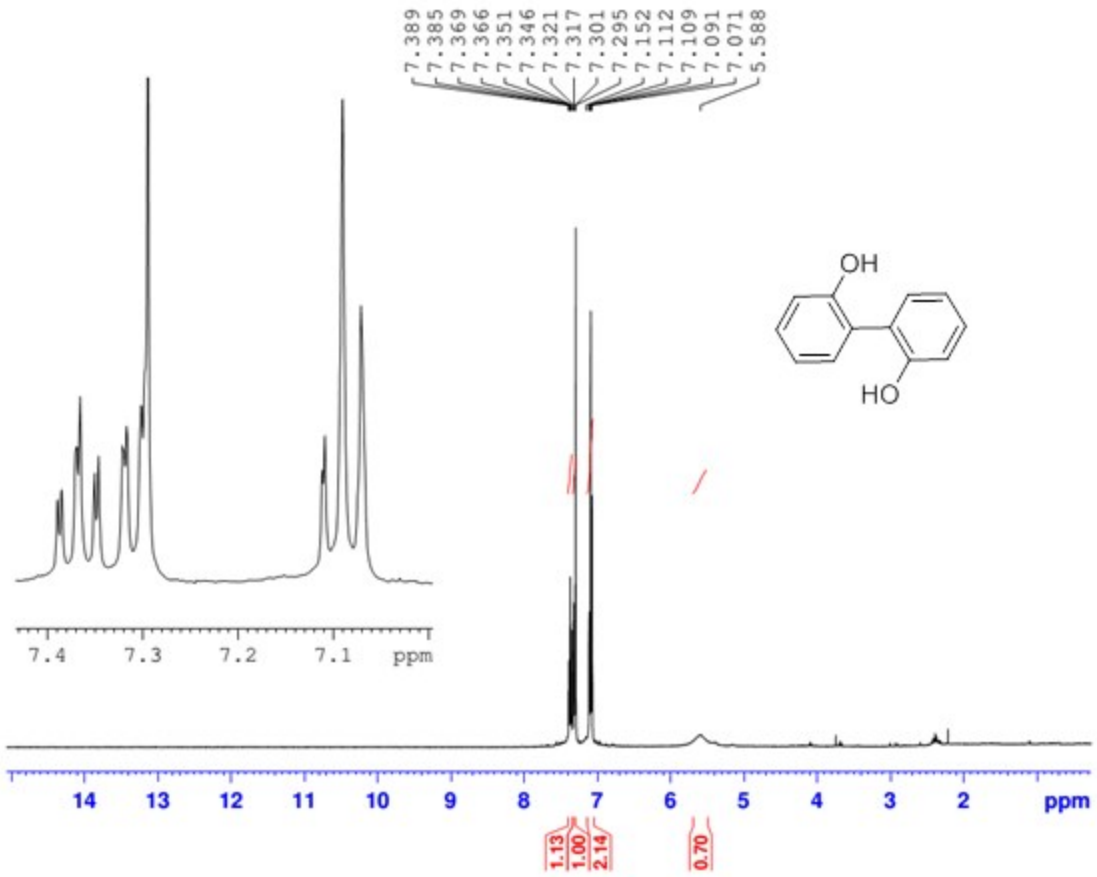

Figure S40. ^{1}H-NMR spectrum (400 MHz, $CDCl_3$) of [1,1'-biphenyl]-2,2'-diol

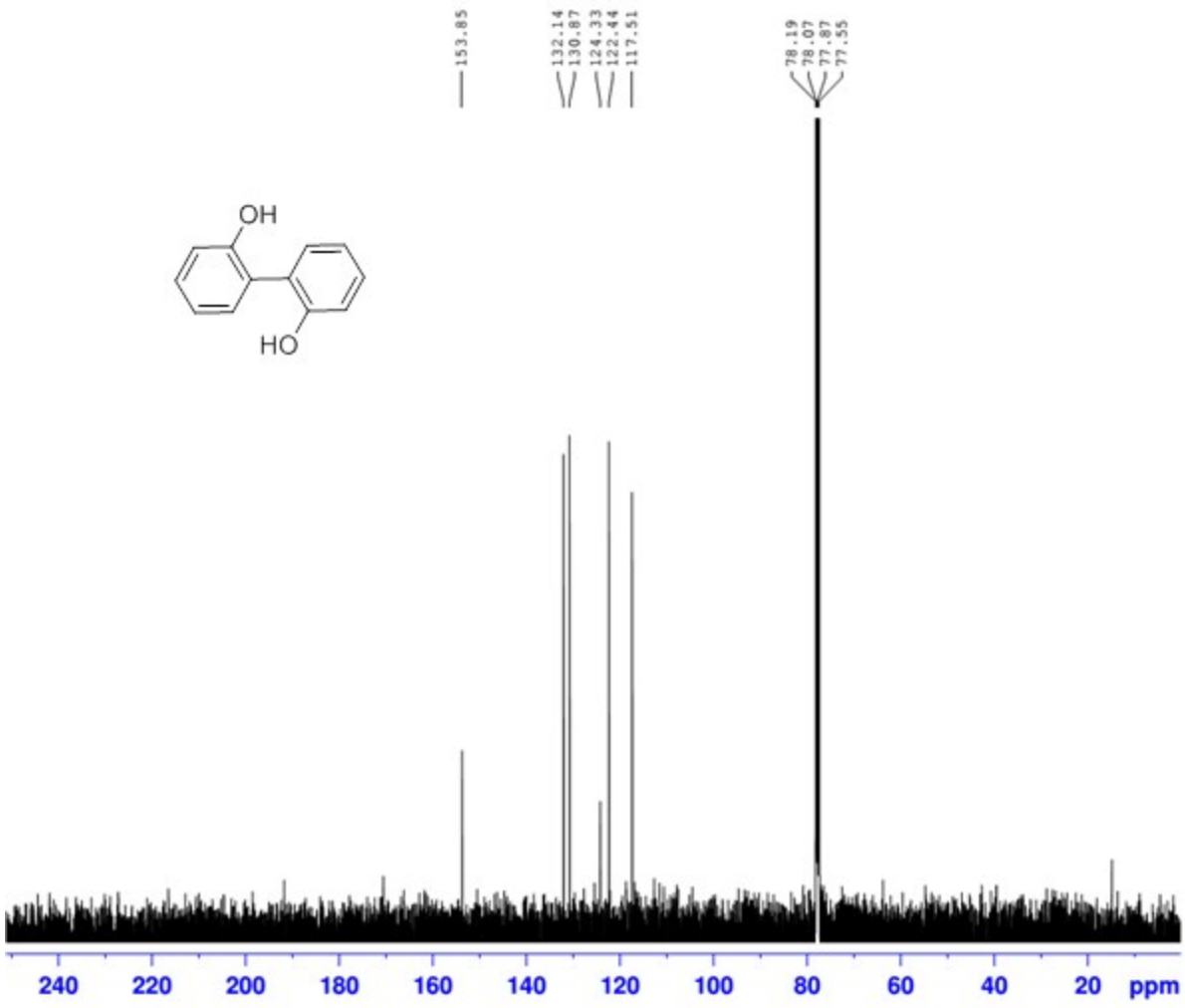

Figure S41. ^{13}C-NMR spectrum (100 MHz, $CDCl_3$) of [1,1'-biphenyl]-2,2'-diol

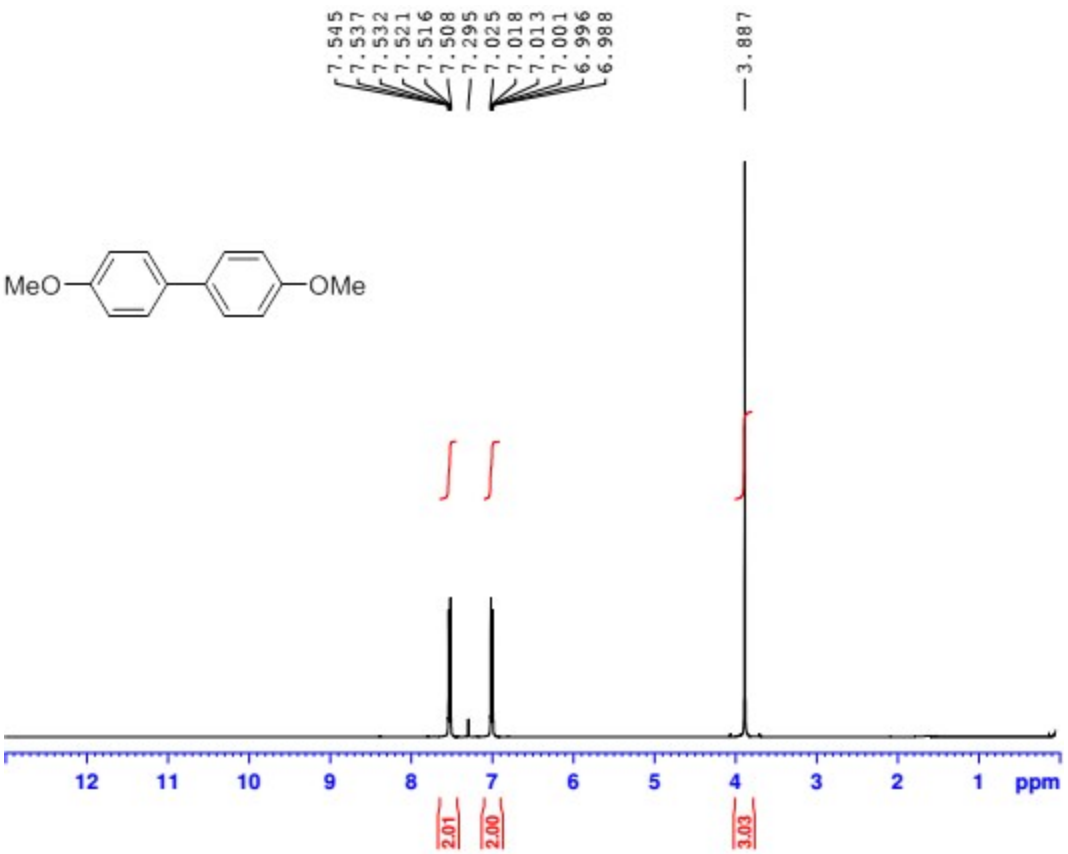

Figure S42. ^{1}H-NMR spectrum (400 MHz, $CDCl_3$) of 4,4'-dimethoxy-1,1'-biphenyl

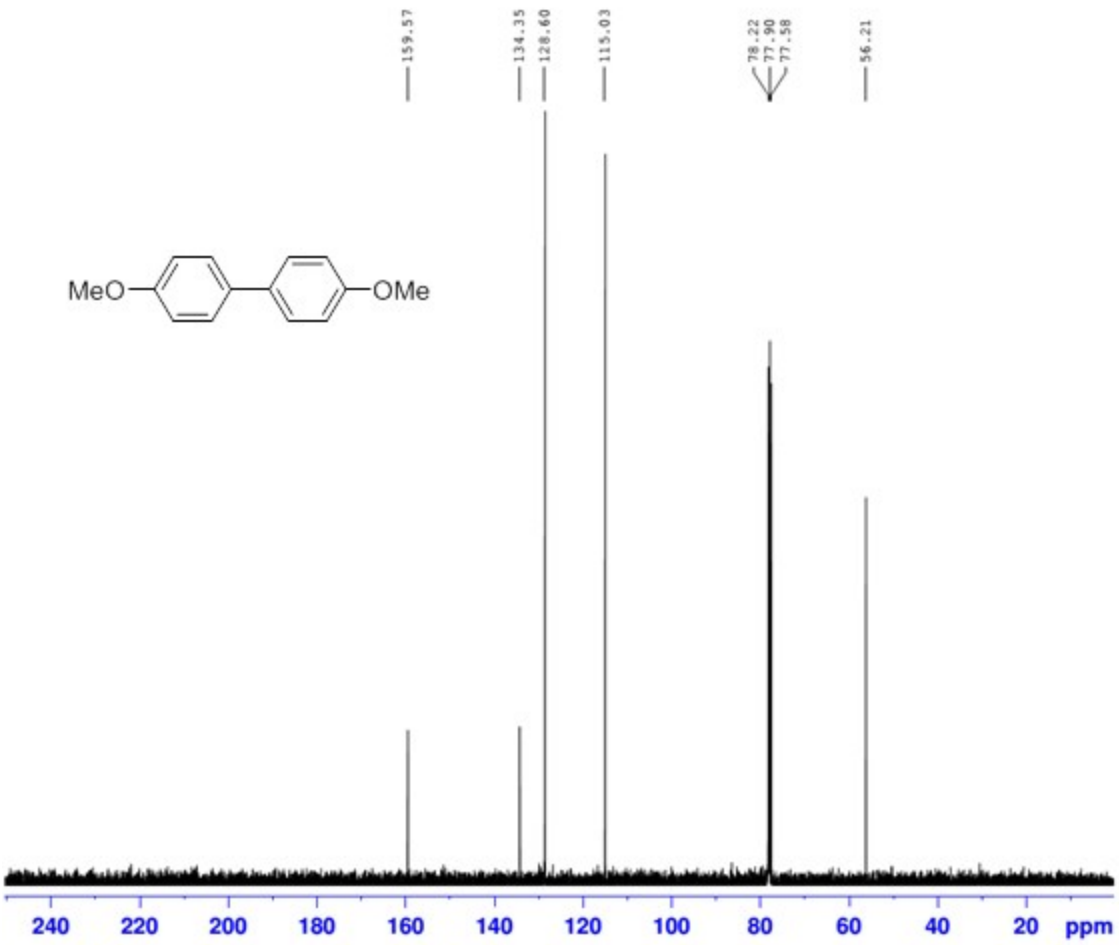

Figure S43. ^{13}C-NMR spectrum (100 MHz, $CDCl_3$) of 4,4'-dimethoxy-1,1'-biphenyl

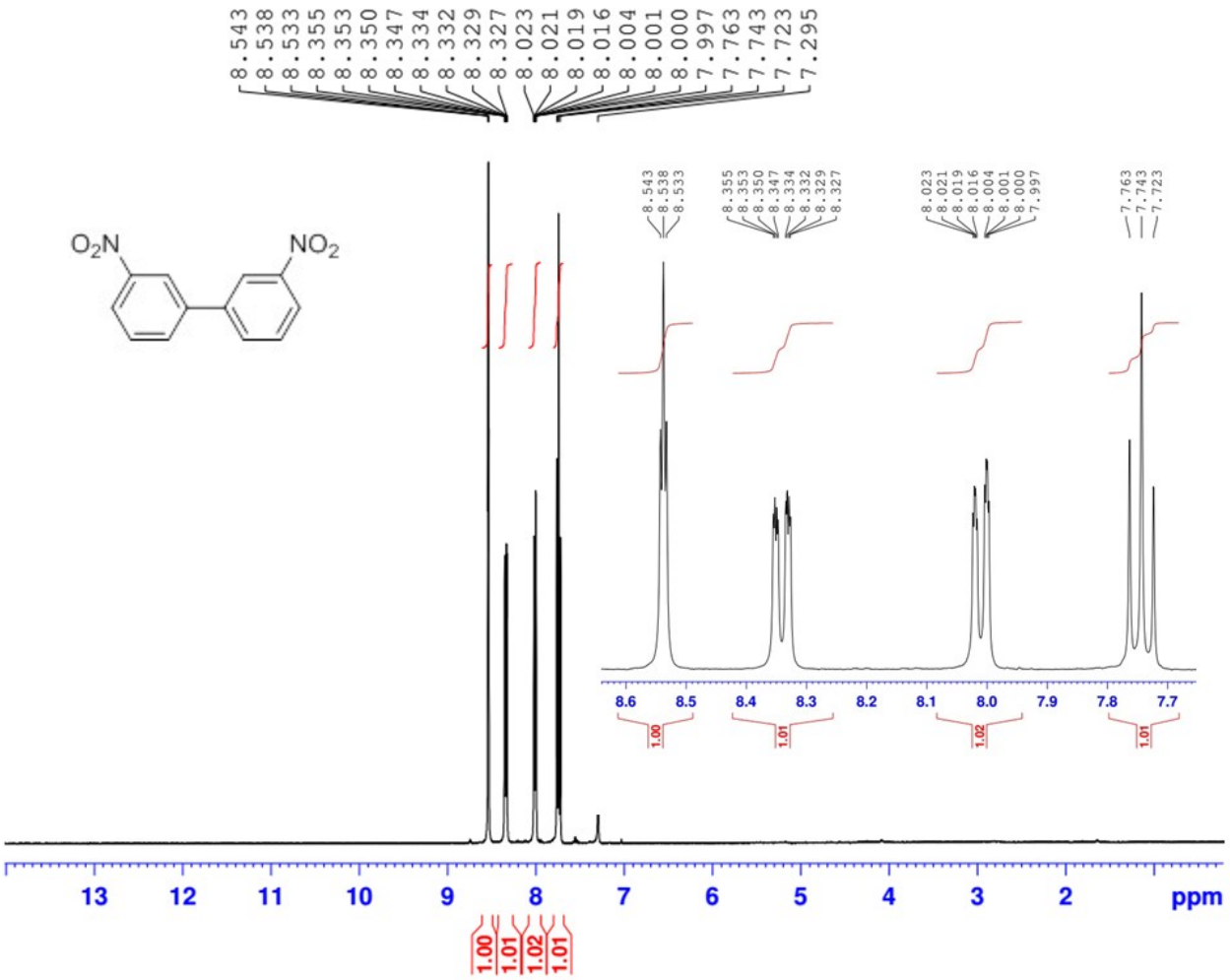

Figure S44. ^{1}H-NMR spectrum (400 MHz, $CDCl_3$) of 3,3'-dinitro-1,1'-biphenyl

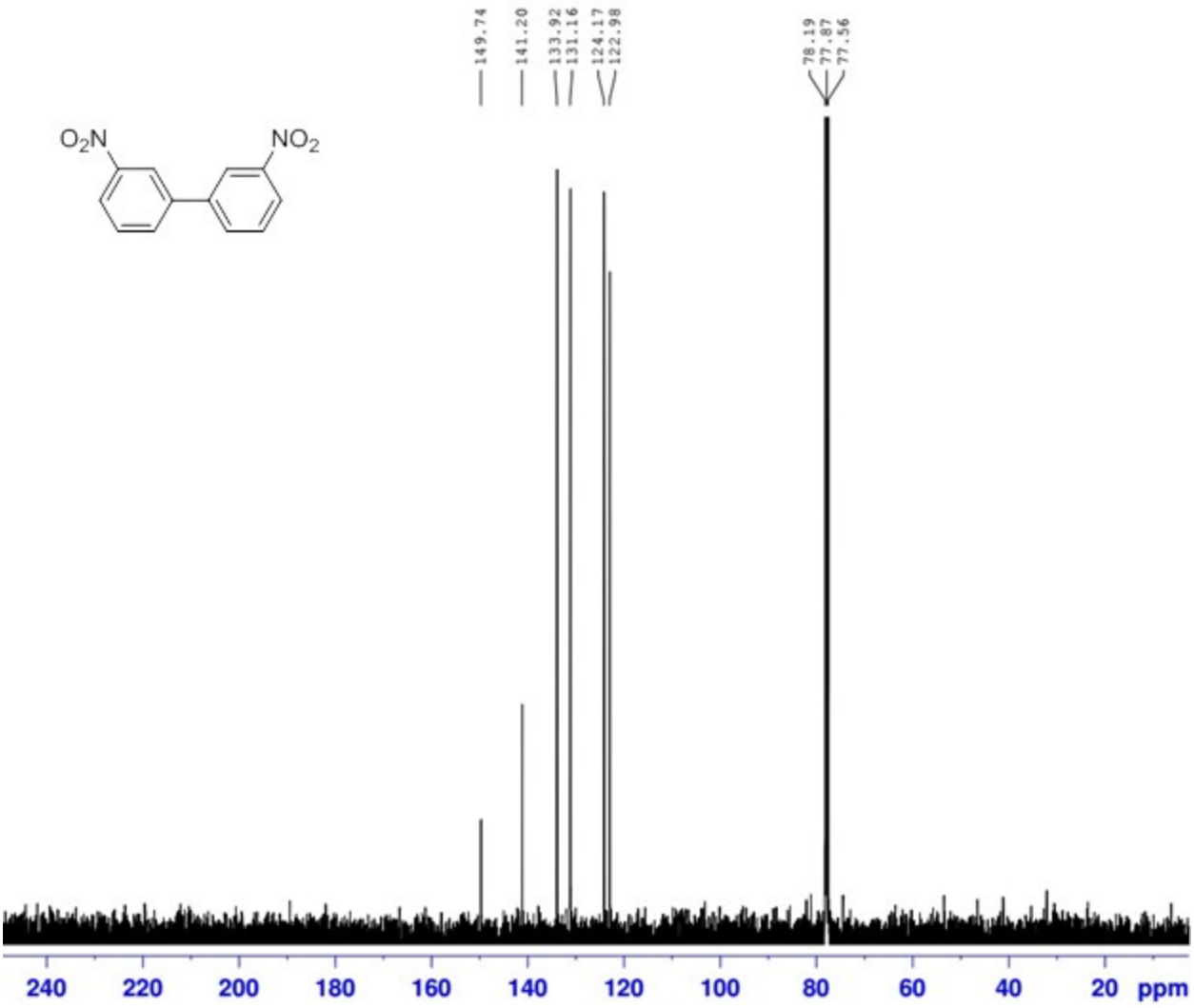

Figure S45. ^{13}C-NMR spectrum (100 MHz, DSMO-d_6) of 3,3'-dinitro-1,1'-biphenyl

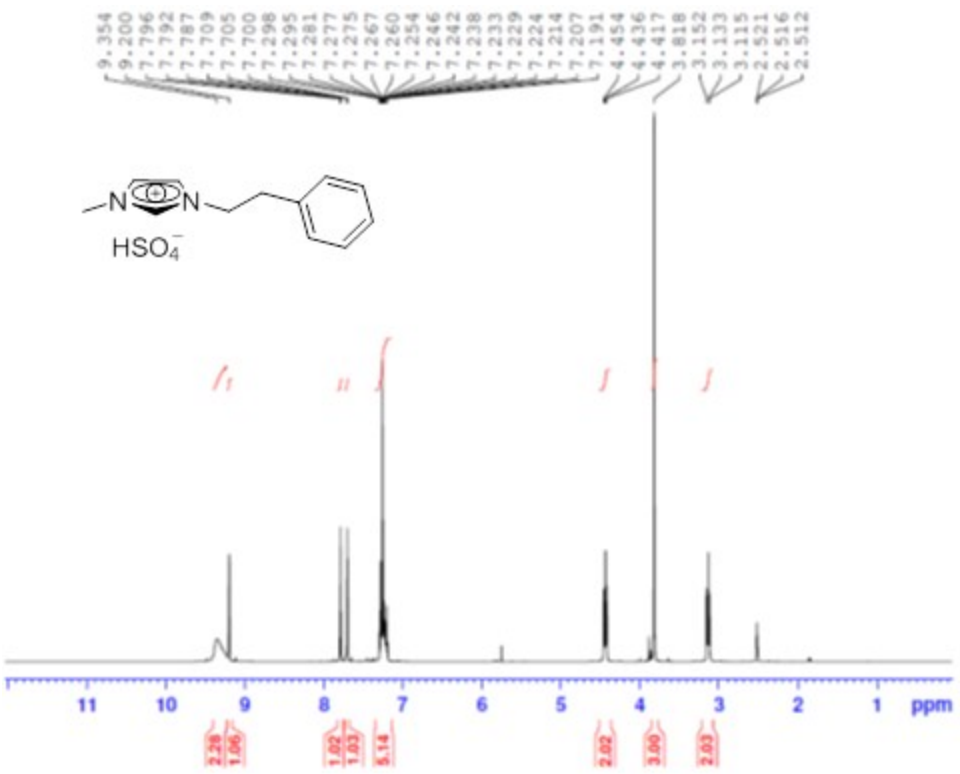

Figure S46. ^{1}H-NMR spectrum (400 MHz, DSMO-d_6) of 1-methyl-3-phenethyl-1H-imidazolium hydrogen sulfate

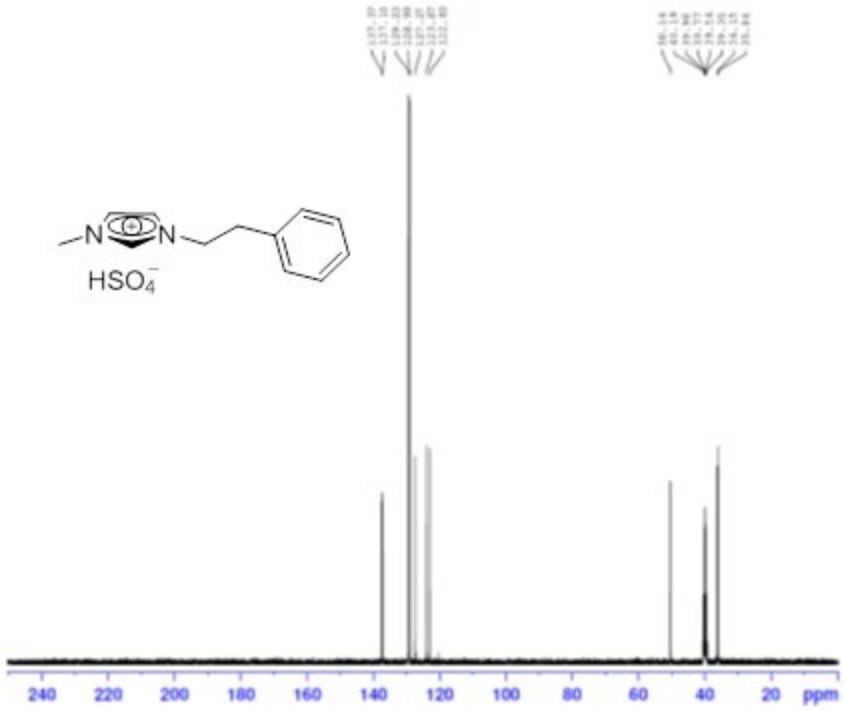

Figure S47. ^{13}C-NMR spectrum (100 MHz, DSMO-d_6) of 1-methyl-3-phenethyl-1H-imidazolium hydrogen sulfate

4. Film